2013

Performance characteristics of ammonia engines using direct injection strategies

George Zacharakis-Jutz
Iowa State University

Performance characteristics of ammonia engines using direct injection strategies

By

George Elias Zacharakis-Jutz

A thesis submitted to the graduate faculty

in partial fulfillment of the requirements for the degree of

MASTER OF SCIENCE

Major: Mechanical Engineering

Program of Study Committee:
Song-Charng Kong, Major Professor
Daniel Attinger
Thomas Brumm

Iowa State University
Ames, Iowa
2013

TABLE OF CONTENTS

List of Tables

List of Figures

List of Equations

List of Terms

ATDC.....After Top Dead Center
BMEP.....Break Mean Effective Pressure
BSEC.....Break Specific Energy Consumption
BSCO.....Break Specific Carbon Monoxide
$BSCO_2$.....Break Specific Carbon Dioxide
BSHC.....Break Specific Hydrocarbon (Unburned)
BSPM.....Break Specific Particulate Matter
$BSNH_3$.....Break Specific Ammonia
BSNOx.....Break Specific Nitric Oxide/Nitrogen Dioxide
BTDC.....Before Top Dead Center
CAD.....Crank Angle Degree
CAD_{Pmax}.....Crank Angle Degree of Max Pressure
CFR.....Cooperative Fuel Research
CI.....Compression Ignition
CO.....Carbon Monoxide
CO_2.....Carbon Dioxide
COV_{Pmax}.....Coefficient of Variance of Max Pressure
COV_{CADmax}.....Coefficient of Variance of Max Pressure Crank Angle Degree
Daq.....Data Acquisition Hardware
DME.....Dimethyl Ether
EPA.....Environmental Protection Agency
HC.....Hydrocarbons (Unburned)
HCCI.....Homogeneous Charge Compression Ignition
LHV.....Lower Heating Value
NH_3.....Ammonia
NOx.....Nitric Oxide/Nitrogen Dioxide
O_2.....Oxygen
P_{max}.....Max Pressure
RPM.....Rotations per Minute
SCR.....Selective Catalytic Reduction
SI.....Spark Ignition
SOI.....Start of Injection
SSAS.....Solid State Ammonia Synthesis

Acknowledgments

A special thanks to Dr. Song-Charng Kong for his guidance and support as major professor. Working in Iowa State University's engines lab has been a great pleasure and I am grateful to Dr. Kong for allowing me to join the team. I am also grateful for his guidance and support over the past two years in my venture to achieve this degree.

I would like to acknowledge the Iowa Energy Center for its financial support in making this project possible. I would like thank Mr. Norm Olsen for his continued support throughout this project.

I would like to thank Dr. Daniel Attinger and Dr. Thomas Brumm for serving on my program of study committee and their advice throughout my time at Iowa State University.

I would like to thank Matthias Veltman, Chris Gross, Jordan Tiarks, Cuong Van Huyng, Aaron Bertram, and the rest of my fellow graduate students who have aided me over the past two years. I would also like to thank Jim Dautremont for his continued support in developing the test apparatus for my experimentation.

I would also like to extend a special thanks to Dr. Kyung Hyun Ryu for his guidance and support over the past year. His collaboration has been instrumental in the success of this project and all projects in the Iowa State University engine lab.

Abstract

In this study performance characteristics of ammonia engines using direct injection strategies are investigated. Ammonia is a carbon-free fuel, and thus its combustion does not produce carbon dioxide, a critical greenhouse gas. Ammonia can be produced by using renewable energy sources (e.g., wind and solar) and used as an energy carrier. Recent research also has shown that the efficiency of solar thermochemical production of ammonia can be increased by combining the ammonia solid-state synthesis cycle with hydrogen production. Ammonia is under consideration for a potential storage method for wind energy. Ammonia's nature as carbon-free and its ability to be renewably produced make it an alternative to fossil fuels.

In this study two direct injection strategies are tested and performance data, and exhaust emissions are recorded and analyzed.

The first strategy tested liquid direct injection in a compression-ignition (diesel) engine utilizing highly advanced injection timings. Ammonia was used with dimethyl ether (DME) in a duel fuel combustion strategy. Ammonia was mixed with DME prior to injection. DME was chosen as a diesel substitute for its close fuel properties to ammonia. Three ammonia-DME ratios were tested: 100%DME, 60%DME-40%NH_3, and 40%DME-60%NH_3. Engine speeds of 1900 rpm and 2500 rpm were used based on the operational capability of 40%DME-60%NH_3.

Operation at 40%DME-60%NH_3 required injection timing ranging from 90-340. Highly advanced injection timings resulted in homogeneous charge compression ignition combustion (HCCI). Cycle-to-cycle variations were reduced with increased load. NOx,

NH_3, CO, CO_2, and HC were reduced with increased load for 40%DME-60%NH_3. Low temperature combustion from low in-cylinder temperature from ammonia vaporization resulted in low NOx emissions meeting EPA emissions standards for small engine operation.

The second strategy tested gaseous direct injection of ammonia in a spark-ignition (gasoline) engine. A CFR engine was operated at idle using the existing gasoline port injection system. Ammonia was directly injected using a solenoid injector. A ruthenium catalyst was implementing to partially decompose ammonia into hydrogen. Testing was performed over a range of seven performance modes using gasoline, gasoline-ammonia, and gasoline-ammonia with ruthenium catalyst. Injection timings of 270, 320, and 370 BTDC were used.

Gasoline-ammonia showed little improvement in break specific energy consumption and CO_2, and exhibited increased levels of NOx and HC over performance modes using gasoline only. Due to ammonia's low flammability limits and slow flame speed combustion efficiency was reduced. With the ruthenium catalyst Improvements in flywheel power were seen over performance modes without catalyst. The peak in-cylinder pressure was increased, and the start of ignition was advanced over both gasoline-ammonia and gasoline only performance modes. There was a significant reduction in NOx and NH_3 present in the exhaust. Hydrogen present in the fuel increased combustion efficiency due to high flammability limits and high flame speed. Improvements in combustion efficiency resulted in reduced CO and HC over both gasoline-ammonia and gasoline only performance modes.

Chapter 1 Introduction

1.1 Motivation

With growing world population come increasing demands for fuels to drive the automotive transportation industry. Currently the transportation industry depends primarily on a petroleum fuel base with a total world usage of refined petroleum products of 88.13 million barrels a day [1]. Dependency on petroleum based fuel presents both immediate and long term issues. Immediate issues concerning petroleum fuels are primarily focused on emissions. Petroleum is predominantly made up of chains of hydrocarbons, which when burned produce carbon monoxide (CO) and carbon dioxide (CO_2) among other products. Both CO and CO_2 are widely attributed in part to a global temperature increase. CO forms the greenhouse gas ozone (O_3) through reaction with oxygen while CO_2 is in and of its self a greenhouse gas. Beyond the immediate issues, fossil fuels (petroleum and natural gas) have an end date, a time when the crude oil and natural gas reserves are depleted. Estimated depletion times vary and will surely be extended as drilling technologies improve, but nonetheless, the time will come when fossil fuels will no longer be a viable option.

Much work has been done in search of alternative fuel sources for transportation vehicles. Among such potential replacements are electrical (battery), biomass-derived fuels (ethanol and biodiesel), and hydrogen fuel sources for vehicles. Each fuel presents a unique challenge to large scale implementation. Batteries have a life span and require special consideration upon disposal. Batteries also, as of current,

present issues with vehicle range and recharge ability as well as use electricity that is primarily generated using carbon based fossil fuels. Ethanol and bio-diesel fuels also present some challenges. The primary concerns of these fuels in that they are also based on carbon chain makeup and therefore contribute to CO and CO_2 pollution. Hydrogen has been tagged by many as the ultimate fuel. Hydrogen has high energy content per unit mass and is easily combustible, and when combusted produces water as the only meaningful byproduct. However, hydrogen presents serious challenges in implementation as a transportation fuel. Although hydrogen is an ideal fuel for internal combustion engines with respect to emissions, hydrogen is very difficult to store. Hydrogen is primarily stored at very high pressures or very low temperature and has a low energy density per unit volume in both methods of storage. Low energy density presents difficulty in implementing hydrogen as an onboard fuel.

There is another less known alternative fuel. Anhydrous ammonia has the potential as a non-carbon based fuel. The chemical makeup of ammonia is three hydrogen atoms combined with a single nitrogen atom meaning combustion results in zero carbon emissions. Ammonia also has a distinct advantage over pure hydrogen in onboard storage. Ammonia is able to be stored at room temperature and minimal pressure in a liquid form. While in a liquid form ammonia has an energy density comparable with gasoline fuel [2]. Ammonia also has the potential to be synthesized from renewable energy sources such as wind and solar. Wind is a particularly appropriate source because ammonia can serve as a method of energy storage during peak output [3]. Ammonia is not without its flaws. Ammonia is a highly corrosive fuel

and therefore requires specific materials (i.e. stainless steel/Teflon) to be used for wetted parts. The material requirements present challenges in obtaining key equipment such as injectors as many components are not commercially available. Ammonia also exhibits a low lower heating value (LHV) and a very high latent heat of vaporization. With the combination of the above factors and a slow laminar flame speed ammonia becomes a challenging fuel for both compression ignition engines and spark ignition engines. The high latent heat of vaporization of ammonia results in combustion chamber cooling when used in liquid direct injection applications such as in common compression ignition engines. The combustion chamber cooling inhibits steady combustion resulting in poor combustion efficiency and limitations in both operating range and performance. When ammonia is used in gaseous port injection strategies the gaseous ammonia replaces inlet air resulting in reduced volumetric efficiency for the engine. Reduced volumetric efficiency limits both operating range and engine performance. In order to counteract the unfavorable fuel characteristics of ammonia duel fuel approaches are often used [4]. However, based on the potential of ammonia it is of interest to further examine methods for combusting ammonia in internal combustion engines, which will expand the operating range and increase the performance of ammonia fueled engines.

1.2 Objective

The objective of this research is to expand the operating range and performance capabilities of internal combustion engines using ammonia by implementing new

injection strategies for fuel delivery. This project modifies existing methods for fuel delivery of ammonia to optimize and expand the engine speed and load limit and performance parameters for both compression ignition engines and spark ignition engines. The existing methods for delivery involve liquid direct injection for diesel engines and gaseous port injection for compression ignition and spark ignition engines, respectively. Liquid direct injection approaches struggle to achieve high concentrations of ammonia due to cooling of the combustion chamber as a result of ammonia's high latent heat of vaporization. And gaseous port injection struggles with reduction of volumetric efficiency. Both methods have potential for improvement. In order to fully optimize the fuel delivery system it is hypothesized that a combination of the two standard fuel delivery approaches is needed. The envisioned system would maximize volumetric efficiency by utilizing direct injection while minimize heat loss due to ammonia vaporization through highly advanced liquid direct injection or gaseous direct injection. Such a system would also strive to achieve maximum level of ammonia in the dual fuel mixture. The purpose of this paper is to explore the results of two such options to increase the load limit when ammonia is used in internal combustion engines. The two methods tested were highly advanced liquid direct injection and gaseous direct injection.

Chapter 2 Theoretical background

The search for alternatives to fossil fuels has extended in all directions. Some of the primary contenders include electrical, biomass-derived fuels (biofuels), and hydrogen fuel sources. Each alternative has inherent issues in their current stage of development. Until battery technologies improve electric vehicle's lack range while deferring emissions to the power plants, most of which are fossil fuel based. Batteries also present environmental issues with proper disposal. Although biofuels are not from fossil resources, they are still hydrocarbon fuels and thus will produce CO and CO_2 in a similar manner as conventional fossil fuels. Moreover, biofuels have hidden greenhouse gas costs in the form of fuel used during planting, harvesting, and processing. Another option is hydrogen fuel systems. Ideally such a system utilizes pure hydrogen which under complete combustion produces only water as a byproduct. Hydrogen also exhibits a great potential for efficiency based on a high LHV or usable energy. The issues of onboard storage and cost of production have limited the feasibility of pure hydrogen operation at present. However, due to the great potential of hydrogen both in performance and emissions, further exploration and solutions are sought for storage and transportation.

2.1 Properties of Ammonia

Ammonia has arisen as a potential hydrogen carrier to solve the problem of on board storage. Although ammonia (NH_3) is not a pure hydrogen compound, it is easily stored in liquid state at a pressure of 10.3 bar. The ability to store ammonia in a liquid state gives ammonia an advantage in energy per unit volume when compared to pure hydrogen. In other words, for equivalent tanks more hydrogen is stored in ammonia (liquid) than in a tank of pure hydrogen (gaseous or liquid). This is best illustrated in Table 2.1 by fuel energy density. Ammonia's storage capabilities demonstrate an advantage over hydrogen as an onboard fuel. Ammonia is also a very competitive fuel when compared to conventional fuels in terms of energy cost, i.e. ¢/MJ. Ammonia is less than one cent higher than gasoline at 3.38 ¢/MJ compared to gasoline and diesel at 2.94 and 2.81 ¢/MJ, respectively. Although ammonia storage has much less energy density than gasoline and diesel, ammonia exhibits significantly higher energy density than compressed natural gas (CNG), liquid hydrogen, and gaseous hydrogen. Ammonia also has a higher octane number than gasoline type fuels, which allows ammonia to be used in higher compression ratio engines. The ability to use ammonia with higher compression ratios allow for more efficient engine operation [5].

Table 2.1 Key fuel properties for various fuels considered for use in internal combustion engines.

Properties	Units	Gasoline	Diesel	Compressed Natural Gas	Gaseous Hydrogen	Liquid Hydrogen	Dimethyl Ether	Ammonia
Formula		C_8H_{18}	$C_{12}H_{23}$	CH_4	H_2	H_2	CH_3OCH_3	NH_3

Lower Heating Value	MJ/kg	44.5	43.4	38.1	120.1	120.1	28.43	18.8
Flammability Limits, gas in air	Vol.%	1.4-7.6	0.6-5.5	5-15	4-75	4-75	3-18.6	16-25
Laminar Flame Speed	m/s	0.58	N/A	N/A	3.51	3.51	N/A	0.15
Autoignition Temperature	C	300	230	450	571	571	350	651
Storage method		Liquid	Liquid	Compressed Liquid	Compressed gas	Compressed Liquid	Compressed Liquid	Compressed Liquid
Storage Temperature	C	25	25	25	25	-253	25	25
Storage Pressure	KPa	101.3	101.3	24,821	24,821	102	500	1030
Absolute minimum ignition energy	MJ	0.14	N/A	N/A	0.018	N/A	N/A	8.0
Octane Rating, RON	RON	90-98	N/A	107	>130	>130	60.6	110
Fuel Density	Kg/m^3	698.3	838.8	187.2	17.5	71.1	668	602.8
Energy Density	MJ/m^3	31,074	36,403	7,132	2,101	8,539	18,991	11,333
Cost	$/gal	3.46	3.88	2.08*	N/A	N/A	N/A	1.45**
Cost per MJ	¢/MJ	2.94	2.81	7.70	N/A	N/A	N/A	3.38
Latent Heat of vaporization	kJ/kg	71.78	47.86	104.8	0	N/A	467	1,369

[4], [6], [5], [2], [7], [8], [9].
*Average cost as of April 2012.
**price conversion from $575 estimated price per ton for 2012, price much higher than previous years.

2.2 Combustion Characteristics of ammonia

As a fuel ammonia also presents many of the upsides of hydrogen. Like hydrogen, ammonia contains no carbon and therefore produces no CO or CO_2. However, unlike hydrogen water is not the only byproduct of ammonia combustion. When ammonia is burned in an unaltered state byproducts include nitric oxide (NO) and nitrogen dioxide (NO_2) both of which are considered harmful pollutants and as a combination (NOx) are regulated by the Environmental Protection Agency (EPA) [10]. The resultant NOx from ammonia combustion is primarily produced from fuel-bound nitrogen which is separated from the hydrogen and seeks to re-bond. The free nitrogen bonds primarily with free oxygen, thus producing NOx. NOx, however, can be converted to nitrogen (N_2) and water (H_2O) using selective catalytic Reduction (SCR). Use of an SCR

can simultaneously reduce NOx and residual ammonia from incomplete combustion in the exhaust. As of current there are, however, no production SCR's available for small vehicle application. Therefore, further development of the industry is needed. Never-the-less the technology does exist to transform ammonia combustion into an essentially nonpolluting event.

There are alternative options, however, to potentially enable clean ammonia combustion. Ammonia can be decomposed before combustion into hydrogen and nitrogen, which in effect results in hydrogen driven engine with byproducts returning to water. Several theoretical studies have been conducted to examine the potential efficiency of a hydrogen operated engine that utilizes onboard decomposition of ammonia [6] [2]. Zamfirescu *et al.* [6] suggested that if all parts of the fuel system were properly utilized the potential efficiency of the entire system could reach 65%. When compared to standard efficiencies of current systems we begin to see the vast potential (~30% and ~35% for gasoline and diesel, respectively). In order to achieve high efficiencies as suggested, a comprehensive engine fuel system must be used. A fully comprehensive system utilizes the cooling properties of ammonia to cool both the engine and the passenger cabin. The exhaust gas is utilized to heat the dissociation catalytic reaction. However, for some applications the exhaust temperature does not reach the necessary temperature (500^{o}C) to decompose ammonia. A solution that has been proposed is to oxidize a portion of the fuel in the exhaust line, which in turn provides the additional heat for the ammonia decomposition to occur [11]. These main implementations combined with the higher efficiency of hydrogen engines results in

highly efficient machines [6]. Using ammonia in a comprehensive engine design fully utilizes the potential of storage capabilities combined with high efficiency combustion and zero pollution of hydrogen. These systems are ideal but are not the only manner for ammonia combustion.

Other studies suggest alternatives, such as using a catalyst to minimally crack or decompose the ammonia resulting in a mixture of ammonia with traces of hydrogen for ignition enhancement purposes. Frigo *et al.* [12] worked with a similar setup using both ammonia and hydrogen to simulate a dissociation catalyst. Using this model in a single cylinder spark ignition engine they were able to achieve engine break thermal efficiencies of nearly 26%. It is also believed that with increased compression ratio the thermal efficiency could be further improved [12]. It should also be noted that this example did not include comprehensive fuel supply and thus did not utilize ammonia cooling or exhaust gas heat, both of which would increase the overall efficiency of the engine.

2.3 Energy Storage for Renewable Electric

Ammonia has upsides beyond storage and emissions. Although ammonia is currently produced from natural gas it also can be produced from any electrical source by utilizing a traditional air separation unit, electrolyzer, and the Haber-Bosch synthesis loop (2.1) [13] [14]. Developed by Fritz Haber and Carl Bosch in 1913, the Haber-Bosch system is currently responsible for 90% of the world ammonia production [14].

$$N_2 + 3H_2 \longrightarrow 2NH_3 \qquad (2.1)$$

The most common form of the Haber-Bosch system utilizes natural gas to produce the hydrogen for ammonia synthesis. However, utilizing other sources of hydrogen allow the Haber-Bosch process to become independent of natural gas. As mentioned, one method is the combination of an air separation unit to produce the nitrogen, an alkaline electrolyzer to produce hydrogen from water, and the Haber-Bosch synthesis loop to combine the hydrogen and nitrogen into ammonia [13].

Further developments have led to more advanced methods for producing ammonia from renewable sources. Solid state ammonia synthesis (SSAS) produces ammonia from air and water as well (2.2), but eliminates the need for electrolyzers and the Haber-Bosch synthesis loop, thus reducing the power input necessary to operate the system.

$$2N_2 + 6H_2O \longrightarrow 4NH_3 + 3O_2 \qquad (2.2)$$

SSAS uses a membrane to directly convert water and nitrogen into oxygen and ammonia thus reducing the power input from 12,000 kWh/ton-NH_3 to 7,500 kWh/ton-NH_3 compared to an electrolyzer/Haber-Bosch system [14] [3]. It is estimated that using the SSAS process would be able to produce ammonia at a cost of 347 $/ton [3]. SSAS presents a very promising and less expensive alternative to the Haber-Bosch synthesis process. Both SSAS and the Haber-Bosch result in several very important implications. First, with proper application of SSAS and Haber-Bosch synthesis ammonia has the potential to be an entirely renewable fuel. If solar, wind, or hydro power were used to

synthesize ammonia then renewable energy would be used to create an onboard fuel that in turn could be used in the manufacturing process of the initial power source. This system has the potential for an entirely renewable power cycle. Furthermore, the pollutant production of the power cycle can be reduced to nearly nothing. The pollutants of renewable energies primarily come from the construction process. Using ammonia properly as a fuel would produce next to zero harmful emissions potentially eliminating harmful pollutants from the power cycle.

Now it is important to understand that the infrastructure for such a grid of renewable electrical sources may not exist. However, ammonia can help build this infrastructure. This leads to the second important implication of creating ammonia from renewable sources. One of the most criticized aspects of solar, wind, and tidal is that there is not always sunlight, wind, and waves. This means that at time these renewable energy sources produce nothing while at other times, when the conditions are right, an excess of electricity is generated. The excess electricity drives down electrical prices and hurts other producers. For example the clearing price for wind being zero ($0.00) due to fuel costs (wind) being zero forces the local power grid prices to also decrease [15]. Storage of the excess energy is the goal so the energy can be reused when electricity is at a shortage.

Viable storage methods are crucial in promoting growth of renewable sources of energy. Ammonia presents such storage mechanisms. Using the excess electricity to synthesize ammonia allows the indefinite storage of the energy. Once the energy is stored in the ammonia it then has several potential uses. As has been discussed

ammonia could be used in commercial vehicles. Ammonia could also be used in industrial size stationary generators allowing the energy to be returned to the grid. And finally the ammonia can be used in its current application as fertilizer for field crops. Ammonia provides an easily stored versatile storage mechanism for renewable electrical sources.

2.4 Existing Infrastructure

Because ammonia is currently used in a high quantity as a fertilizer, at a rate of 8.4 million tons in 2006 with trends showing increase [16], there is existing infrastructure and distribution (primarily in the Midwest). U.S. geological survey estimates that a total of 13.8 million tons of ammonia were used for various applications in the U.S. in 2011, with 136 million tons used worldwide [8]. Furthermore, ammonia is a commonly handled substance and therefore ammonia handling knowhow is common and understood. Having existing storage and distribution infrastructure gives implementing ammonia as a commercial fuel an advantage over other alternative fuels that require entirely new infrastructure such as hydrogen.

2.5 Limitations of Ammonia

Up to this point many of the upsides of ammonia have been discussed but ammonia does present some challenges as a commercial fuel. Although ammonia is currently $575 per ton (2012 estimate [8]) it is as said synthesized from natural gas. In order to fully take advantage of ammonia it needs to be synthesized from renewable

electrical sources. Electrically synthesizing ammonia does present a cost increase. This then may cause the price of ammonia to exceed that of conventional fuels such as gasoline or diesel. Ammonia also presents practical mechanical challenges. Ammonia is a highly corrosive fuel and therefore requires specific materials (i.e. stainless steel/Teflon) to be used for wetted parts. The material requirements present challenges in obtaining key equipment such as injectors as many components are not commercially available. Ammonia also presents problems from a combustion stand point. Achieving theoretical values experimentally is often the most difficult task.

Ammonia has several difficult obstacles to overcome before it becomes more viable. The first is a very high latent heat of vaporization (1370 kJ/kg), which represents the energy required to complete the transition from a liquid state to a gaseous state. In practical terms it is seen that if ammonia is exposed to atmospheric pressure from its traditional storage pressure (10.3 bar), the vaporization of the liquid ammonia can cause freezing of the surrounding environment. A very high latent heat of vaporization presents several problems when planning an ammonia combustion system. The first limiting factor, to a high latent heat of vaporization, is the massive cooling effect the fuel has when introduced to the combustion chamber, which inhibits combustion and can cause misfire. This is especially present if direct injection of liquid ammonia is used [4]. The high latent heat of vaporization also has implications when planning a fuel delivery system, especially if the fuel system utilizes gaseous ammonia. Since ammonia is stored in a liquid state in order to deliver gaseous ammonia, vaporization must occur. The vaporization at a high rate may cause cooling or even freezing of the storage bottle.

The cooling effect causes the pressure in the bottle to decrease, which restricts the fuel flow and can starve the engine. Therefore, any fuel delivery system has to account for the cooling effects of ammonia vaporization.

The second drawback of ammonia as a fuel is the energy content or the total usable energy. In more technical terms the higher heating value (HHV) represents the total possible energy obtained from combustion of a given fuel. The lower heating value (LHV) represents the total usable energy produced during the combustion of a fuel. Because both the HHV and more importantly the LHV of ammonia are much less than those of conventional fuels (Table 2.1), more fuel ammonia is required to produce the same power when compared to other fuels on a mass basis.

The final limiting factor of ammonia as a fuel is the relatively slow flame speed and limited flammability limits of ammonia. Ammonia exhibits an extremely slow laminar flame speed on the order of four times less than that of gasoline [5]. A slow flame speed limits operation ability of engines using ammonia with respect to engine speed in rotations per minute (RPM). The low flammability limits of ammonia also restrict the operational range of ammonia. Ammonia exhibits a lower limit of 15 percent of gas in air, which when compared to gasoline, 4.7, is high [5]. The flammability limitations also cause restriction on the aspiration design of ammonia driven engines (Full throttle limitations discussed in more detail in Chapter 3).

Not all the limitations of ammonia are considered entirely negative. The effects that are considered negative can be transformed into potential bonuses of using ammonia as a fuel. The most notable of such is utilizing the high latent of vaporization

of ammonia to cool both the passenger compartment and the engine. The hot engine coolant would also prevent pressure loss from rapid cooling of the ammonia tanks. The utilization of this technique is a helpful edition in dramatically increasing the overall efficiency of the engine [6].

2.6 Liquid Ammonia Direct Injection

Dating back to as early as Word War II Ammonia has been used as a supplement fuel in times of fuel shortages [17]. When first used, and for many subsequent tests and trials, ammonia has been used in diesel fuel application [18] [19] [20]. Ammonia has often been seen as a diesel type fuel in part because of the high octane number. In addition due to the low LHV of ammonia liquid direct injection is advantageous to supply a large amount of fuel. Due to the properties of liquid direct injection the issues of low energy fuel content can be controlled as no inlet air is displaced by fuel.

However, the disadvantages of ammonia as a liquid direct injection fuel may outweigh the benefits. By using direct injection method ammonia is injected in a liquid state and as injection occurs ammonia begins to vaporize, thus drawing heat from the cylinder. This, the high latent heat of vaporization, causes dramatic cooling of the cylinder head inhibiting high combustion efficiency [4]. This becomes an extremely important issue on startup of the engine when engine temperatures are already low. Furthermore, ammonia has an extremely high auto-ignition temperature (651°C), which then requires the use of a pilot fuel in order to initiate combustion [6]. For diesel applications this requires either a dual fuel approach such as ammonia and dimethyl

ether or double injectors. The dual fuel approach requires specific fuels to operate and fuel ratio is limited to approximately sixty percent ammonia for such dual fuel systems. Studies have also shown that combustion efficiency is sacrificed in these methods due to heat loss and slow flame speed [4]. Pilot fuel injection approaches require dual injectors, tanks, and delivery systems that may offer their own challenges. An alternative method of delivery is desired that utilizes the benefits of diesel type systems while adverting the negative effects.

2.7 Gaseous Ammonia Port Injection

Other approaches have been tested regarding ammonia fuel delivery. A very common and simple to implement method is port injection of ammonia as either a primary or secondary fuel. In such setups the fuel is delivered in a gaseous state into the intake port along with the air [21]. Port injection of gaseous ammonia eliminates the cylinder chamber heat loss due to vaporization of ammonia. There are, however, downsides to port injection of ammonia. The ammonia displaces air delivered to the combustion chamber thusly reducing the air volumetric efficiency of the engine as demonstrated by Equation 2.3.

$$\boldsymbol{e_v = \frac{2\dot{m}_a}{\rho_i V_d N}} \qquad \textbf{(2.3)}$$

Where, $\dot{m}_a$ is the mass of air inducted into the combustion chamber, ρ_i is the density at the intake manifold, V_d is the displacement volume, and N is the engine speed. It is also necessary to have an additional ignition source for port injection of gaseous ammonia

much like diesel application. Often this is gasoline or hydrogen. An additional charge is needed because the absolute minimum energy required to ignite ammonia is nearly one hundred times greater than that of gasoline [5]. Ammonia also exhibits a relatively slow flame speed therefore an additional charge of gasoline or hydrogen helps propagate combustion through the combustion chamber. Studies have replaced gasoline with hydrogen in order to reduce the amount of non-ammonia fuel in the mixture. Using hydrogen as an ignition charge also reflects the potential of using an ammonia dissociation catalyst to crack ammonia into partial hydrogen. If a catalyst was used the system would become a single fuel system.

Chapter 3 Experimental Setup

The scope of this study is to examine alternative fuel delivery methods for ammonia to increase the operating range and performance capabilities. In an attempt to expand the operating range two methods were tested.

The first was aimed at modification of a diesel type application. In this case a standard dual fuel mixture of ammonia-dimethyl ether (DME) was used and reconfigured to operate with highly advanced injection timing, resulting in homogeneous charge compression ignition (HCCI) conditions. This strategy uses highly advanced direct injection timings in order to disperse the cooling effect of ammonia over a greater time period. HCCI retains the majority of the direct injection benefits seen in the diesel applications. The injection occurs late in the intake stroke or early in the compression stroke resulting in little reduced loss in air volumetric efficiency. Fuel delivery issues are also adverted by liquid injection allowing sufficient fuel delivery in a short period of time. And finally a high compression ratio was attained (20:1) allowing for increased efficiency.

The second approach tested was aimed at increasing the operating range of spark-ignition engine applications. This system utilized direct injection of gaseous ammonia into a gasoline engine with a slightly increased compression ratio. This design was aimed at utilizing all the benefits of diesel type systems while eliminating the heat loss problem due to latent heat of vaporization. An ammonia dissociation catalyst was also implemented in this system in order to increase the engine performance

capabilities. An alternative pressurization system was utilized that theoretically uses waste exhaust heat to provide energy to the storage bottle.

Both setups are discussed in detail in their respective sections. First highly advanced liquid ammonia direct injection operation conditions will be discussed followed by the discussion on gaseous ammonia direct injection.

3.1 Liquid Ammonia Direct Injection for CI Engine Application

To use ammonia in a direct injection diesel engine, ammonia is mixed with dimethyl ether (DME) which serves to initiate combustion. DME is necessary to compensate for ammonia's high resistance to autoignition. DME is considered a viable diesel substitute, which also exhibits similar properties to that of ammonia thus allowing for a non-separating fuel mixture. The properties of ammonia and DME are compared with other engine fuels in Table 2.1.

The original setup used for the exploration of highly advanced liquid ammonia direct injection was designed very similar to a diesel direct injection system. A fuel combination of ammonia and DME was directly injected into the engine, using conventional to slightly early diesel injection timings. However, it was observed that using conventional injection timings (5-10^{o}CA BTDC) or even earlier injection timings (20-50^{o}CA BTDC) was insufficient to achieve ammonia content in fuel higher than 40% [4]. Thus, in an attempt to increase the operating range and maximum percent of ammonia in the fuel, highly advanced injection timings were used (90-340^{o}CA BTDC). These highly advanced injection timings transform conventional diesel combustion into

HCCI combustion. The highly advanced injection allows the heat loss due to the vaporization of the ammonia to be mitigated over an extended time period thus reducing the negative effects. The experimental setup and test procedure is detailed below.

3.1.1 Engine Stand Apparatus

A Yanmar L70V single-cylinder, direct-injection diesel engine (Table 3.1) was used in this study. The engine test stand consisted of a heavy-duty steal frame to which the engine and dynamometer were mounted. A Klam K10C electromagnetic retarder was used to load the engine. The engine and retarder were coupled directly utilizing a vibration damping flexible tire shaft coupling. To accommodate the unit, a few modifications to the cylinder head were also made. A new injector, a glow plug, a cylinder pressure sensor, and thermocouples to measure cylinder head temperature and intake air temperature were installed in the cylinder head.

Table 3.1 Yanmar engine specifications

Engine Model	Yanmar L70V
Engine Type	Air Cooled, Four Stroke, Compression Ignition
Combustion Type	Direct Injection
Type of Aspiration	Natural Aspiration
Bore x Stroke (mm)	78 x 67
Compression Ratio	20:1
Total Displacement (cm^3)	320
Valves per Cylinder (Int./Exh.)	1/1
Rated Speed (rpm)	3600
Rated Power (kW)	4.3
Injection System	Electronically controlled
Injection Pump	External Pump
Injector	Bosch high pressure gasoline direct injection (GDI)

3.1.2 Injection System

The engine required significant modifications to the injection system for this research. A Bosch fuel injector designed for use in gasoline direct-injection (GDI) engines was installed using the pre-existing injector port. The original injection system was replaced by an electronically controlled fuel system to overcome material incompatibilities and to realize flexible injection timing. The new system consists of an electronic injector, a common-rail, an air-operated high-pressure piston pump, and a Compact-Rio real-time controller. The GDI prototype injector has a maximum pressure capability of 210 bar, which is significantly lower than that of modern diesel fuel injection systems but is sufficient to atomize fuel since ammonia and DME vaporize quickly due to their considerably high vapor pressures.

3.1.3 Fuel Delivery and Storage System

During the test, the fuel mixture was drawn from the mixture tank by an air-operated high-pressure piston pump. The pump pressurized the fuel to the desired injection pressure of 206 bar. During injection, fuel was passed through a common rail to eliminate pressure waves from the pump. A Compact-Rio real-time controller was used to monitor the crankshaft position, cam shaft position, and rail pressure to ensure accurate injection timing and injection duration. Fuel mixing was done in a two part process. First each fuel was transferred into respective holding tanks from their original bottles. This process was done using pressure driven flow, as the original bottles are pressurized. Once the holding tanks were filled the fuel was transferred into the mixing tank. The mixing tank was placed on a scale and one fuel at a time was fed into the tank

using the pressure difference to drive the flow. The scale was used to get an exact measurement by mass of the fuel mixture ratio (NH_3/DME). Once the desired mixture was achieved the tank was manually mixed. The mixing tank directly fed the air-operated high-pressure piston pump.

3.1.4 Data Collection Hardware/Software

The cylinder pressure for combustion analysis was measured using a Kistler 6125B piezo-electric pressure transducer together with a Kistler 5010 charge amplifier. The cylinder pressure was measured every 0.1 crank angle degrees and averaged over 250 engine cycles.

Intake air was drawn from the room and the consumption was measured using a Meriam laminar flow element equipped with a surge air tank, which was mounted below the engine. A computer-controlled single tubular heating element with a nominal power output of 1.1 kW was installed along the centerline of the surge tank and was used to heat the intake air up to 90°C to help counter heat loss due to the high latent heat of vaporization of ammonia. Figure 3.1 shows a detailed schematic of the full test apparatus used for this experimentation.

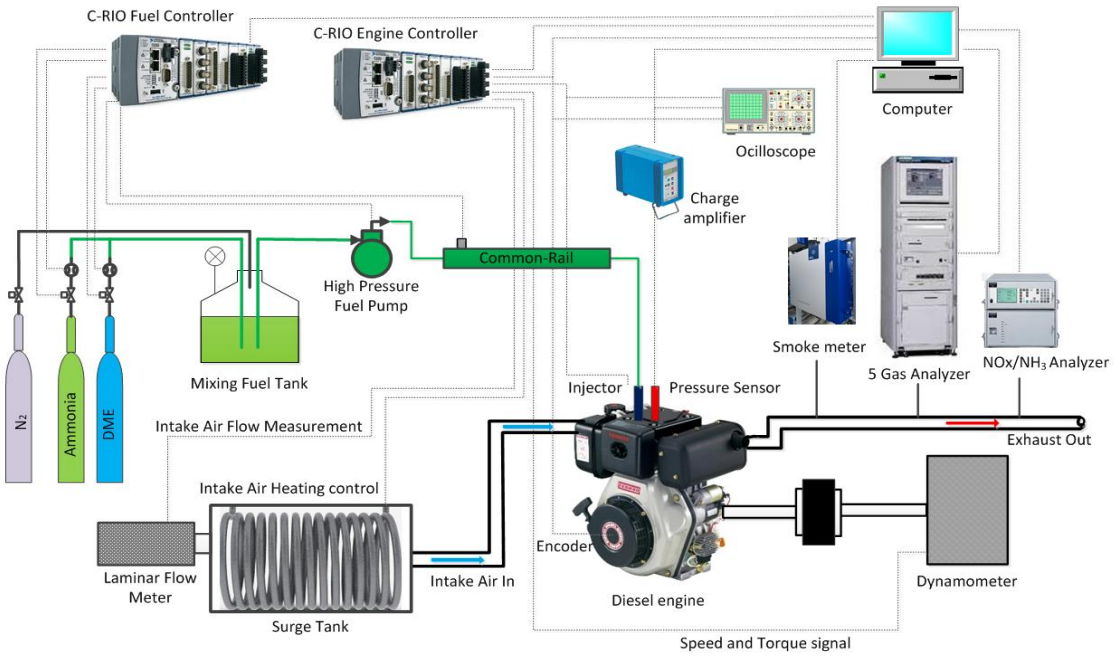

Figure 3.1 Schematic of test apparatus for highly advanced liquid ammonia direct injection testing

3.1.5 Emissions Analysis

The gaseous emissions were measured using a combination of a Horiba MEXA 7100DEGR, Horiba MEXA 1170NX, and DeJAYE emissions analyzers, which have been widely used in industry for studying diesel exhaust emissions as well as the performance of selective catalytic reduction (SCR) systems utilizing urea injection. The emissions data recorded included ammonia (NH_3), nitric oxide and nitrogen dioxide (NOx), carbon monoxide (CO), carbon dioxide (CO_2), hydro carbons (HC), and oxygen (O_2). In particular, exhaust ammonia emissions were measured using a Horiba MEXA 1170NX analyzer and a DeJAYE analyzer, both of which are capable of measuring ammonia and NOx emissions simultaneously. The combination of analyzers used for the NH_3/NOx emissions was due

to failure of the MEXA 1170NX analyzer part way through the data collection process. Proper measures were taken to ensure the replacement analyzer (DeJAYE analyzer) was properly calibrated for the range of emissions present. The smoke number was measured using an AVL 415S soot meter as seen in Figure 3.1.

3.1.6 Test Procedure

In order to investigate the performance characteristics using different fuel mixtures, various injection timings, injection pressures, and intake air temperatures were explored in advance. The engine was also tested at different speed and load conditions. Preliminary tests show that the use of ammonia will limit the load range, and high speed and load operations cannot be attained. Thus, the test conditions are chosen at low to medium loads at engine speeds of 1900 rpm and 2500 rpm. It was also found that high injection pressure and high intake air temperature are required for fuel mixtures with high ammonia content. For instance, an injection pressure of 150 bar and intake air temperature of 60˚C are appropriate for using 100%DME, and 180 bar and 80˚C for 60%DME-40%NH_3. However, operations using 40%DME-60%NH_3 require even higher injection pressure and intake air temperature. Therefore, for all the operations using different fuel mixtures in this study, the injection pressure and intake air temperature were held constant at 206 bar and 90˚C, respectively. The high intake air temperature was needed to compensate the cooling due to ammonia vaporization.

During experiments, the engine was started on 100%DME and allowed to warm up before switching the fuel line to the desirable fuel mixture. For the subsequent testing, the engine was operated at each mode for extended time to allow temperature

to reach steady state prior to data recording. Performance parameters were recorded over a period of time and are presented in the final result as an average value.

3.2 Gaseous Ammonia Direct Injection for SI Engine Application

A Cooperative Fuel Research (CFR) engine was used to investigate gaseous ammonia direct injection in a spark ignition engine in order increase the operating range and performance capabilities. In order to increase the operating range of a gasoline type engine using ammonia, a direct injection system for gaseous ammonia was developed. By implementing a direct injection system over the conventional port injection systems the air volumetric efficiency of the engine may be preserved. There are challenges to implementing such a system. Conventional systems use the storage pressure of the ammonia to drive the injection flow. Direct injection, on the other hand, must have a higher pressure in order to successfully deliver fuel. There were several potential strategies to achieve higher pressure for the gaseous ammonia. The first attempt involved using a liquid pump to pressurize the ammonia then passing the ammonia through a heating element to vaporize the ammonia before injection. This original plan involved a high pressure pump and a regulating valve to set the injection pressure. Although the original setup was able to reach sufficiently high injection pressures the injection pressure was erratic due to highly variable vaporization patterns. Attempts were made to stabilize the vaporization but no sufficient progress was made. There was also the factor that the pump and regulator design was unpractical to implement on

small gasoline engine systems. Therefore, alternative pressurizations systems had to be explored.

An alternative to using a pump and regulator system was to heat the ammonia tank directly. Heating the tank directly increased the vapor dome pressure and then the gaseous ammonia could be siphoned of the top of the tank. Instead of using a pump and regulator to control the pressure it could be directly controlled by maintaining the tank at the desired temperature to achieve the desired pressure. It was found that this method had a much higher ability to control and maintain a steady injection pressure. Moreover, the heated tank method eliminated many hardware elements and significantly reduced the cost of the injection system. This is especially valuable because ammonia compatible hardware is expensive and difficult to obtain for small applications. The injection system used for this experimentation as well as the implementation of the ammonia cracking unit is discussed in Chapter 3.2.3 Fuel Delivery/Storage System.

3.2.1 Engine Stand Apparatus

This experiment utilized a CFR engine with a set compression ratio of 10:1 and constant speed of 1800 rpm. More detailed specifications for the CFR engine are shown in Table 3.2. The CFR engine was an appropriate choice for use in this experiment for several reasons. The CFR is a standardized engine and therefore these results will be standardized as well. The CFR engine was also desirable because it is extremely durable, which is beneficial when working with the corrosive properties of ammonia. The CFR engine is also coupled with a single speed induction type dynamometer. There are

several downsides to using the CFR engine for this testing, which include limited locations for implantation of injector, high friction, and little throttling control. There was only one location to insert an injector and that location had to be shared with a Kistler pressure transducer for measuring cylinder pressure. To achieve mounting, an adapter was created that housed both the pressure transducer and the injector. There were sacrifices in this mounting plan that included an extended passage for the fuel to travel before it reached the combustion chamber. The consequence of the extended passage is flow restriction and delay between injector firing and fuel reaching the combustion chamber. Both these effects are difficult to quantify but are discussed with respect to effect on results in greater detail at a later point.

Table 3.2 CFR engine specifications

Engine Model	CFR Fuel Research Engine
Engine Type	Liquid Cooled, Four Stroke, Spark Ignition
Combustion Type	Direct Injection
Type of Aspiration	Natural Aspiration
Bore x Stroke [mm]	82.5 x 114.3
Compression Ratio	10:1
Total Displacement [cm^3]	611
Valves per Cylinder [Int./Exh.]	1/1
Rated Speed [rpm]	1800
Injection System	Manifold injection
Injection Pump	Bosch
Injector	Bosch type
Injection opening pressure [bar]	82
Fuel injection timing	50 deg ATDC on the intake stroke

3.2.2 Injection System

Gasoline is injected into the intake port with a Bosch type gasoline injector during the intake process. The opening pressure of gasoline injector is 82 bar and injection timing of gasoline is 50 deg ATDC on the intake stroke. A Bosch type fuel pump driven by the CFR research engine was used in this study. The amount of gasoline is manually controlled by the micrometer attached to the fuel pump.

In order to inject directly gaseous ammonia into the CFR engine, a Parker Series 9 Pulse Valve injector was used in this experiment. The injector is a standard solenoid valve injector with 11.2 watt, 28VDC coil and a max pressure of 52 bar. The Series 9 valve injector has a response time of as fast as 160 microseconds with an orifice diameter of 0.039 inches. The Series 9 valve injector is driven by a National Instruments Compact-Rio 9022, a solid state relay, and a variable voltage source. The entire setup was controlled by an in-house designed LabView program. The Series 9 pulse valve injector was an appropriate candidate as an injector based on response time, pressure capabilities, material of wetted parts, and cost. The Series 9 had sufficient response time to act as an injector for the constant speed 1800 rpm CFR engine. 52 bar was also a sufficient max pressure for the purpose of this experimentation. However, most importantly the Series 9 was an in production option that was made of stainless steel and other ammonia compatible materials.

Ammonia was transferred through a 3/8 inch stainless steel line from the holding tank to the injector. Due to the heating of the holding tank to establish sufficient pressure, the injection line had to be heated to prevent the ammonia from condensing

as it cooled. The heating of the injection line was achieved with heating tape controlled by a variable voltage source and regulated by in-line K-type thermocouples.

When the ammonia dissociations catalyst was added, the injection line required modification. 50 grams of 2% ruthenium on 1/8 inch alumina pellets served as the ammonia decomposition catalyst. The catalyst pellets were housed in cylindrical sample tube that was preceded by an identical test tube containing heat exchanging wiring. The whole assembly was placed in the engine exhaust line as seen in Figure 3.2 which maintained exhaust temperatures above 800°C. The exhaust heat exchange was used to both demonstrate the use of exhaust temperature reuse and because other means of reaching such high temperatures were much more difficult to implement. Little information is available on necessary residence time and surface area of catalytic material for ammonia decomposition application. Therefore, specification of the size of the catalyst element was dictated by the space available in the engine exhaust line.

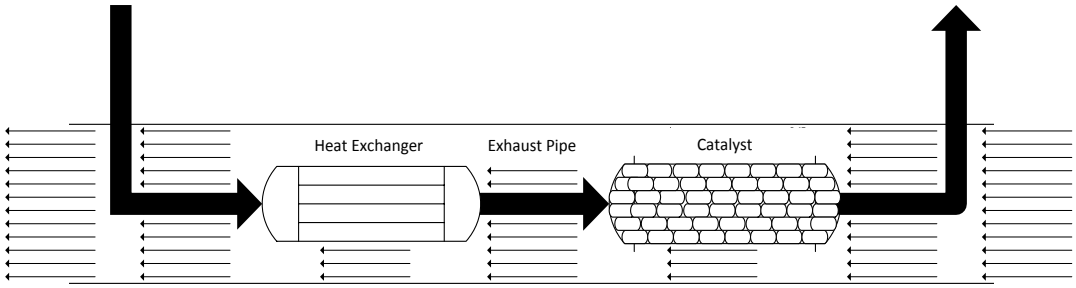

Figure 3.2 Ammonia dissociation catalyst assembly

3.2.3 Fuel Delivery/Storage System

Due to ammonia's toxicity it is necessary to place the storage tank within a well-ventilated cabinet as seen in Figure 3.3(a). The storage tank was a portable stainless

steel vessel with feed in for filling and a feed out to the injection line as seen in Figure 3.3(b). The tank was placed in a hot water bath with a clip on heating element to provide the necessary heat to the tank for achieving desired pressure. The temperature of the water bath was manually adjusted to control the pressure of the holding tank, which was measured using a standard pressure gauge. Both the tank and heating bath were placed on a Mettler Toledo scale in order to measure the ammonia fuel used during testing. The lines leading to and from the tank were made of flexible hosing and looped (Figure 3.3(b)) in order to allow the tank to move freely up and down as to not disrupt the scale reading. The storage tank used for the majority of the experimentation had a pressure limit of 14 bar.

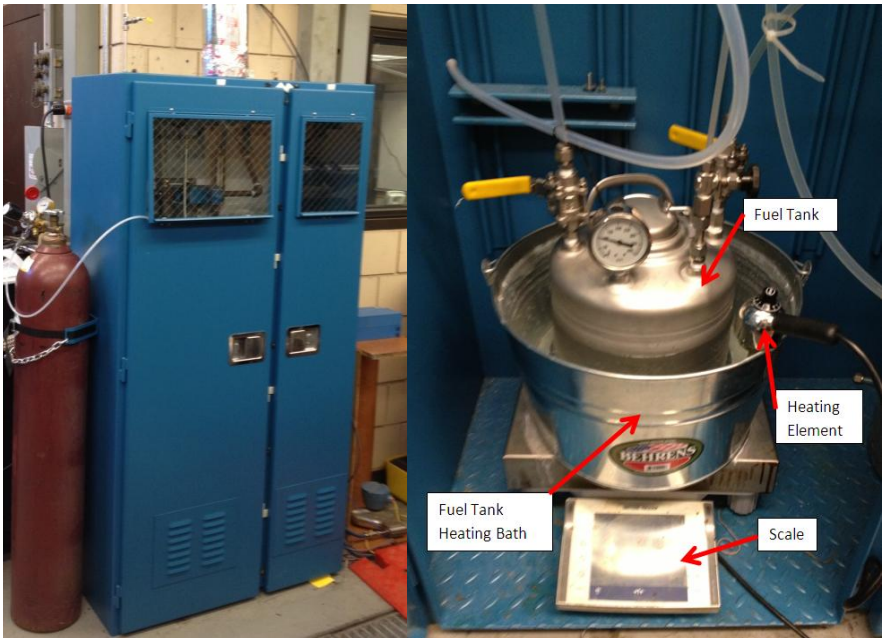

(a) Storage cabinet (b) Holding tank

Figure 3.3 Ammonia storage cabinet and holding tank

3.2.4 Data Collection Hardware/Software

A full schematic for the test apparatus is detailed in Figure 3.4. The engine parameters were collected by a LabView program built to receive and store operating specifications. A National Instrument PCI-6259 data acquisition system was used to obtain data signals. The data collected and stored included most notably pressure traces, heat release rates (HRR), flywheel power, and exhaust temperature. For a full list of data collected in this experiment see Table 3.3. The cylinder pressure for combustion analysis was measured using a Kistler 6052CU20 piezo-electric pressure transducer together with a Kistler 5010 charge amplifier. The cylinder pressure was measured every 0.25 crank angle degrees. Intake air was drawn from a supercharged surge tank and the consumption was measured using an orifice manometer equipped with a 2^{nd} stage surge air tank.

Both ammonia and gasoline consumption rates were taken from Mettler Toledo scales, and injection pressure and temperature of the ammonia was also recorded along with injection timing and duration. See Table 3.3 for a full list of test parameters.

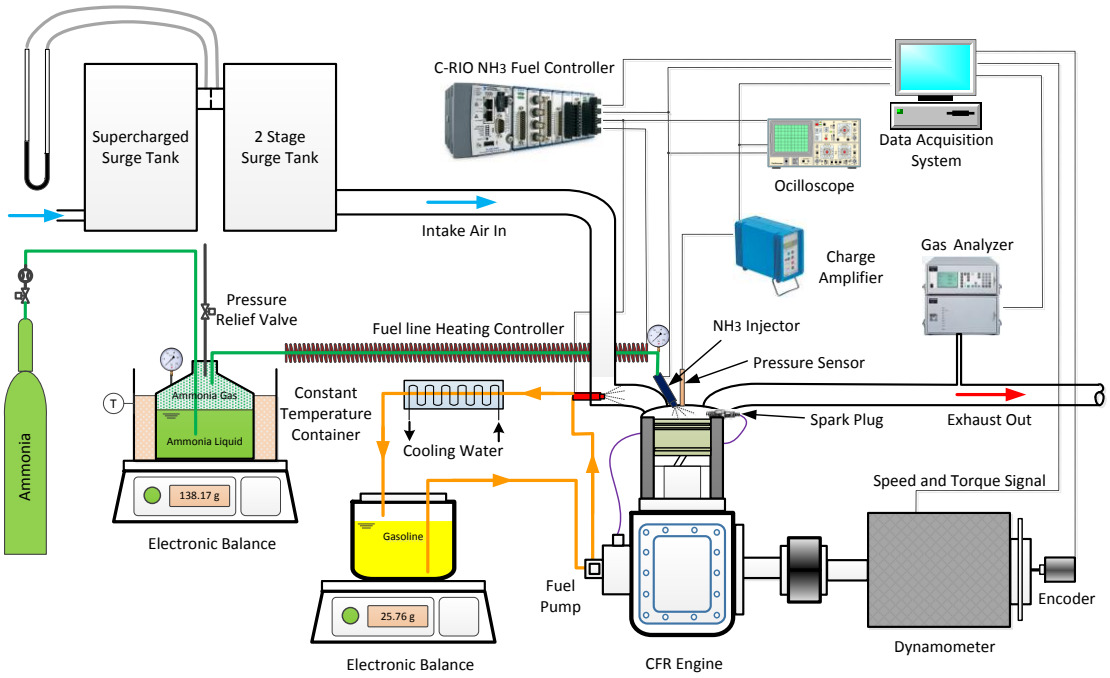

Figure 3.4 Schematic of test apparatus for gaseous ammonia direct injection testing

Table 3.3 Data collected during testing

Measurement	Units	Collection Method
Start of Injection	CAD BTDC	Manually Recorded
Injection Duration	ms	Manually Recorded
Engine Speed	rpm	Daq
Flywheel Power	kW	Daq
Exhaust Temperature	deg C	Daq
Surge Tank Temperature	deg C	Daq
Manifold Pressure	PSIa	Daq
Injection Temp	deg C	Manually Recorded
Injection Pressure	PSIa	Manually Recorded
Fuel Consumption Gas	g/min	Manually Recorded
Fuel Consumption NH3	g/min	Manually Recorded
Air Consumption	min/0.25lb	Manually Recorded
NH3	ppm	Exported to Notebook Doc
NOx	ppm	Exported to Notebook Doc
CO	%-v	Exported to Notebook Doc
CO2	%-v	Exported to Notebook Doc
HC	ppm	Exported to Notebook Doc
O2	%-v	Exported to Notebook Doc

3.2.5 Emissions Analysis

The exhaust gas emissions were measured using a combination of two DeJAYE analyzers, which directly saved emissions data to a notebook file. That data was then able to be exported to an excel file for analysis. The analyzers were contained on a portable emissions analysis cart. The hot exhaust gas was passed through a water knockout unit, which consisted of a heat exchanging element, cooler, and water collection trap. The exhaust emissions of interest were ammonia (NH_3), nitric oxide and nitrogen dioxide (NOx), carbon monoxide (CO), carbon dioxide (CO_2), hydro carbons (HC), and oxygen (O_2). NH_3, CO, CO_2, and HC were measured using infrared while NOx and O_2 were measure using chemical cells.

3.2.6 Test Procedure

As described in Table 3.4 each test was performed over 2 minute durations to average fuel consumption and exhaust emissions. A thirty second period was allowed before each test to allow the outgoing readings to stabilize. Before and after each test using ammonia a baseline test using only gasoline was performed to ensure that unseen changes from day to day testing did affect results. Such parameters as manifold pressure, air tank pressure, engine speed, gasoline injection pressure, gasoline injection timing, ammonia injection pressure, and spark timing were kept constant across all testing. Other parameters were adjusted to create a comprehensive parametric study. These parameters included ammonia injection temperature, gasoline consumption, ammonia injection timing, and ammonia injection duration. The ammonia injection temperature was changed as a result of the addition of the catalyst and therefore were

not included as participant in the parametric study. Thus, the gasoline consumption, ammonia injection timing, and ammonia injection duration were used to create a triple parametric study to determine the optimal operating conditions for the gaseous ammonia direct injection system. The ranges of each of these parameters as seen in Table 3.4 were determined prior to the start of testing as the acceptable range in which the engine would operate.

Table 3.4 Test conditions for gaseous ammonia direct injection testing

	Test Parameter	Value or range	Unit
Constant Test Conditions	Manifold Pressure	1.01	bar
	Air Tank Pressure	2.75	bar
	Engine Speed	1800	RPM
	Ammonia Injection Pressure	13.8	bar
	Spark Timing	30	CADBTDC
	Test Duration	2	Minutes
	Gasoline injection pressure	8.2	MPa
	Gasoline injection timing	30	deg BTDC
Variable Test Conditions	Injection Temperature	40-217	°C
	Gasoline Fuel Consumption	26.5-32.5	g/min
	Ammonia Fuel Injection Duration	8.75-26	ms
	Injection Timing	270-370	CADBTDC

1) Gasoline/Ammonia Base Data

The first set of data that was collected was a full triple parametric study adjusting all three parameters across the full range. The gasoline consumption was varied based on power output beginning with the minimum gasoline level at which the engine would run with consistent firing, which will be referred to as idle. Four total

cases were chosen incrementally staggered from idle to approximately sixty percent of full load. For each case of load from gasoline the injection timing of the ammonia charge was set at 270, 320, and 370 crank angle degrees (CAD) before top dead center (BTDC). At this point it should be noted that injection timing no longer fall in the range of direct injection. This is because in order to see appreciable improvements in performance these early injection timing were necessary. The implications of the early injection timings will be discussed later in more detail. Finally, for each of the three injection timings the injection duration was varied from 10-26 milliseconds in increments of 4 milliseconds. The resulting data was then analyzed to show the performance parameters of the injection system. This set of base testing was also used to prepare performance test parameters as described in the next section.

2) Performance Data

Once base testing was complete and the engine performance data had been examined a set list of conditions was determined as the optimal injection timing and duration of ammonia to reach specific loads. The optimal injection timing and duration along with the corresponding power outputs are listed in Table 3.5. For this second round of data collection the gasoline was kept at idle position to achieve the desired loads the injection timing and duration were set to optimal position, which will be referred to from here on as performance modes. To compare the results to a pure gasoline system, the same performance modes were also achieved using only gasoline. The performance modes were then compared side by side as further discussed in the results section.

Table 3.5 Performance data points for gaseous ammonia direct injection testing

Injection Timing (^{o}CA BTDC)	Injection Duration (ms)	Load (kW)
Idle-Gasoline Only	Idle-Gasoline Only	0.65
320	8.75	1.25
320	9.5	1.50
320	11	1.75
370	12	2.00
370	14	2.25
370	17	2.50
370	23	2.75

3) Catalyst data

The intention of adding the ruthenium ammonia dissociation catalyst was to increase the operating condition of the engine compared to regular ammonia injection. Therefore, in order to test the benefits of adding the ammonia dissociation catalyst the performance modes were replicated using equal gasoline consumption, injection timing, and injection duration as was used in the ammonia performance modes (from Table 3.5). Then to examine the benefits of adding the dissociation catalyst the power output with and without the catalyst were compared.

Chapter 4 Results and Discussion

4.1 Liquid Ammonia Direct Injection for CI Engine Application

The engine was tested using three ammonia/DME fuel mixtures: 100%DME, 60%DME-40%NH_3, and 40%DME–60%NH_3 (by mass). For each fuel mixture three operating loads were tested with the exception of 60%DME-40%NH_3, where four operating points are included. 80%DME-20%NH_3 is also mentioned with respect to the operating range but this mixture is not discussed in detail as it has very similar performance characteristics to 100%DME. All operations were performed at 1900 rpm with several cases at 2500 rpm. This value was chosen based on the maximum operating speed of the 40%DME-60%NH_3, which was the highest ammonia concentration. The slow flame speed and resistance to autoignition of ammonia limits the operating speed, thus all mixtures were operated at 1900 rpm in order to allow for a meaningful comparison between the mixture levels.

4.1.1 Performance Characteristics

At each operating point, different injection timings were successfully tested. It is observed from Figure 4.1 that the injection timing for successful engine operations needs to be advanced as the ammonia content in the fuel mixture increases. The appropriate injection timing range for 100%DME is 0 to 30 BTDC, where the specific timing depends on the engine speed and load. At 80%DME-20%NH_3 and 60%DME–40%NH_3, the operating ranges of injection timing are 5 to 35 BTDC and 20 to 50 BTDC, respectively. Advanced timings are required to achieve stable combustion using

ammonia because ammonia's high latent heat of vaporization and high resistance to autoignition result in increased ignition delay. Furthermore, for 40%DME-60%NH_3, injection timing of 90 to 340 BTDC is necessary for successful engine operation to achieve desirable power output. This means that in order to achieve stable combustion using 40%DME-60%NH_3, highly advanced injection timings must be used, resulting in HCCI combustion characteristics. At such high ammonia concentration the engine is unable to run at conventional diesel injection timings due to in-cylinder air cooling and slow chemistry.

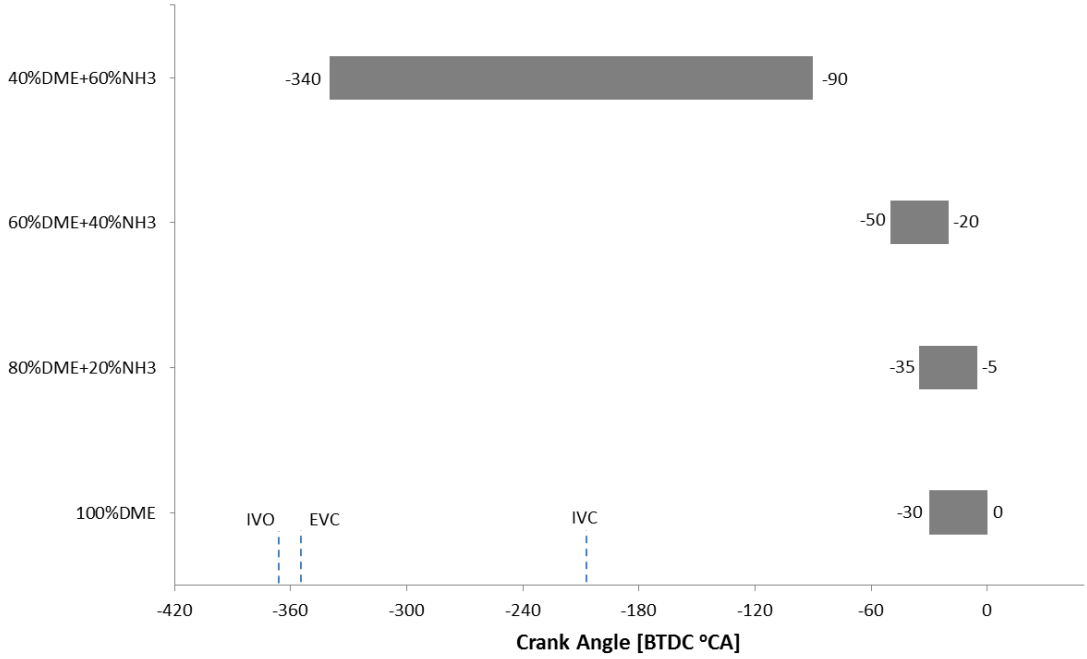

Figure 4.1 Range of possible injection timing for successful combustion using different DME-ammonia fuel mixtures

4.1.2 Pressure and Heat Release Rate Histories

In-cylinder pressure histories, overlapped for multiple consecutive cycles, are presented in Figures 4.2-4.6 for 1900 rpm cases. For 100% DME, 60%DME-40%NH_3, and 40%DME-60%NH_3, the progression of the pressure traces with respect to increased

engine load is presented. Additionally for 40%DME-60%NH_3 the progression with respect to injection timing is presented. Data for the peak pressure and corresponding crank angle are also presented. Note that not all the experimental conditions are presented in Figures 4.2-4.6. Selected data are shown to highlight the effects of fuel composition and injection timings on combustion characteristics. For the 100%DME conditions, shown in Figure 4.2, the engine is very stable at the conditions tested, thus only one load condition (0.28 MPa BMEP) is shown. The peak pressure is approximately 55 bar occurring at 5 ATDC. Results at different load conditions using 100%DME exhibit similar characteristics.

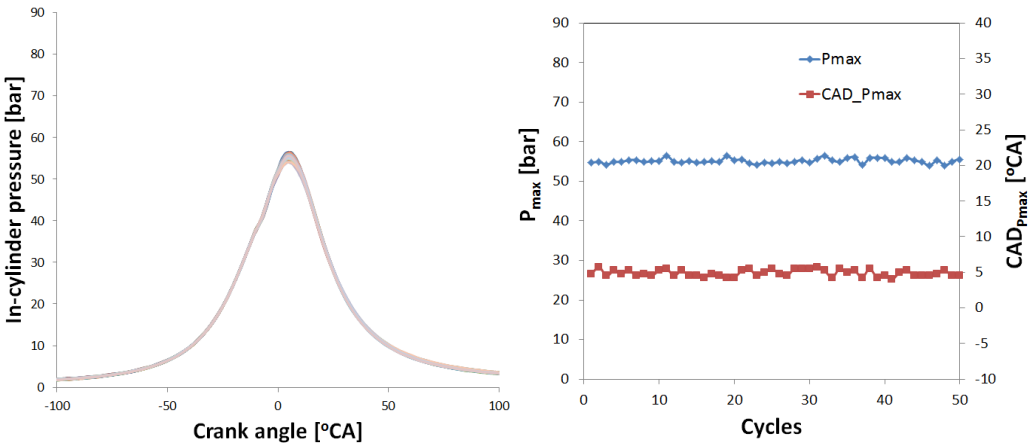

Figure 4.2 Cylinder pressures for multiple firing cycles and the histories of peak pressure and corresponding crank angle for 100%DME, SOI=10 BTDC, BMEP=0.28 MPa

In Figure 4.3 it is seen that for 60%DME-40%NH_3 the variations of peak pressure and CAD_{Pmax} are significant relative to those of 100% DME but are still considered stable. As the engine load increases, the variability of pressure history, peak pressure, and CAD_{Pmax} increases. Additionally, the peak pressure is reduced, and CAD_{Pmax} is delayed

with the increase in engine load. It is believed that at the same injection timing the ignition delay is longer due to the increased quantity of ammonia needed to achieve the higher engine loads. This is caused by the increased temperature loss due to the greater volume of ammonia being vaporized, which can result in more incomplete combustion.

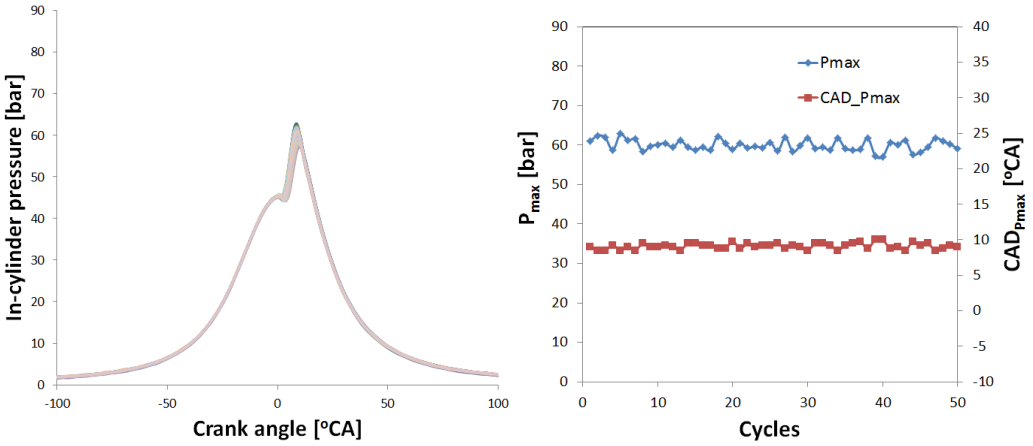

(a) BMEP=0.14 MPa

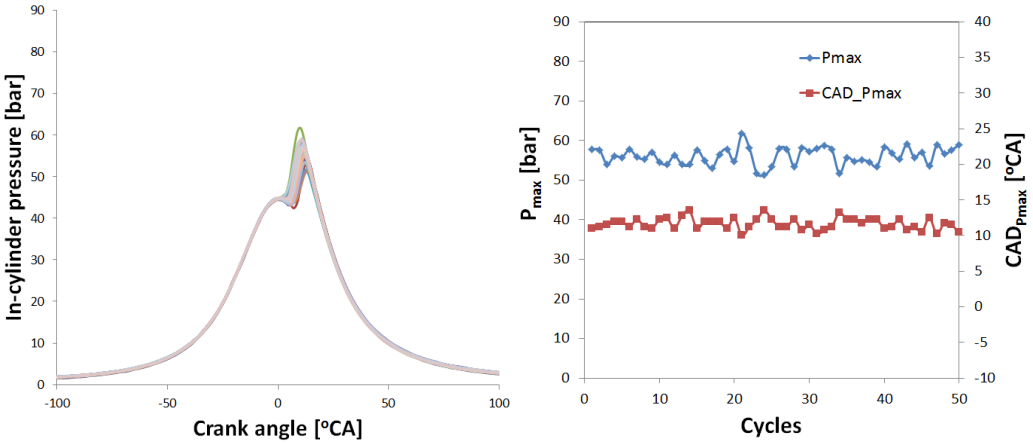

(b) BMEP=0.21 MPa

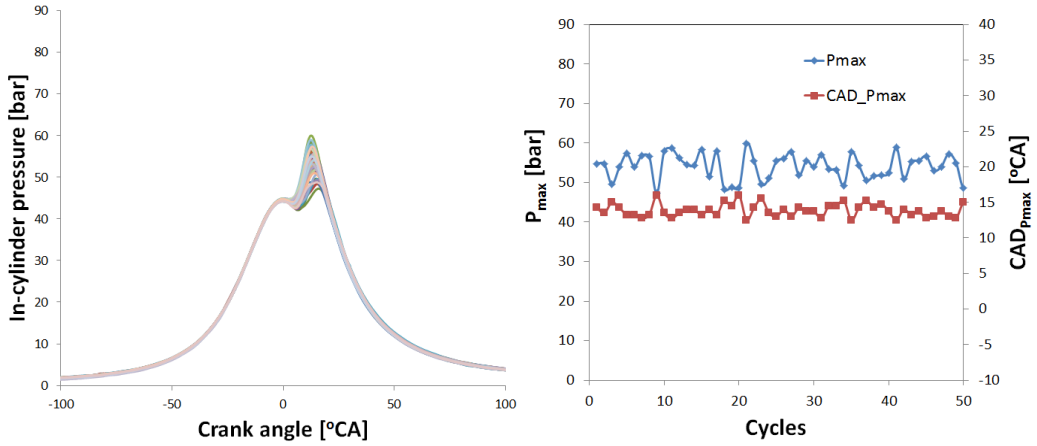

(c) BMEP=0.35 MPa

Figure 4.3 Cylinder pressures for multiple firing cycles and the histories of P_{max} and CAD_{Pmax} for 60%DME-40%NH_3, SOI=20 BTDC

Figures 4.4-4.6 show the pressure history, peak pressure, and CAD_{Pmax} for 40%DME-60%NH_3 with a start of injection (SOI) of 160, 180, and 330 BTDC, respectively. 40%DME-60%NH_3 requires considerably earlier injection timing than 100% DME due to increased ignition delay caused by additional heat loss from high concentrations of ammonia. At an SOI of 160 BTDC, extremely high cycle-to-cycle variation is seen at low load and to a lesser extent at medium load (see Figure 4.4(a) and Figure 4.4(b)). However, from Figure 4.4(c), it is observed that with increased load, the cycle-to-cycle variations are dramatically reduced. Additionally, with increased engine load the peak pressure experiences an increase and CAD_{Pmax} is slightly advanced. It is believed that at high load conditions using very early injection timing (160 BTDC), the increased amount of fuel energy can help achieve stable HCCI combustion.

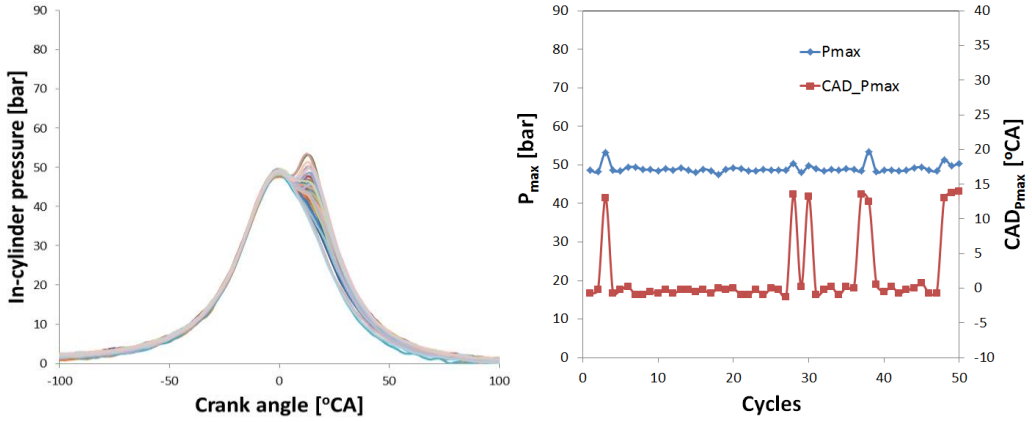

(a) BMEP=0.14 MPa

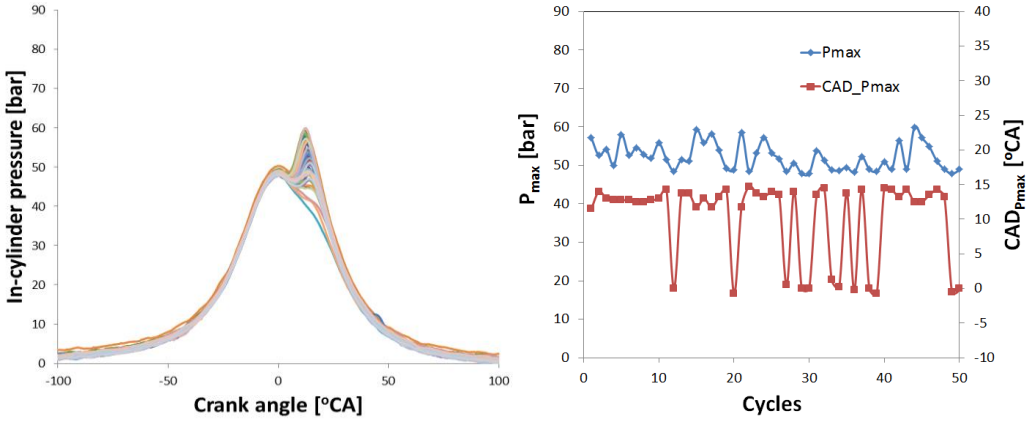

(b) BMEP=0.21 MPa

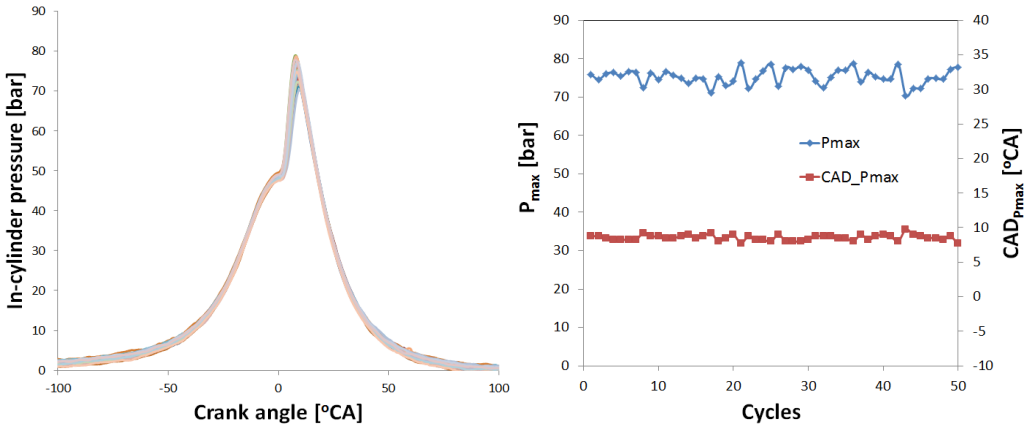

(c) BMEP=0.28 MPa

Figure 4.4 Cylinder pressures for multiple firing cycles and the histories of P_{max} and CAD_{Pmax} for 40%DME-60%NH_3, SOI=160 BTDC

The cycle-to-cycle variation with respect to injection timing is further examined for 40%DME-60%NH_3. Results demonstrate a high sensitivity to not only engine load but also to injection timing, as seen in Figures 4.5 and 4.6. Results show that cycle-to-cycle variation decreases as the injection timing is advanced. It is also observed that the likelihood of misfires is also reduced by using extremely early injection timing as demonstrated by the decreased variation in CAD_{Pmax}. The greatest difference is seen in the transition from SOI at 160 to 180 BTDC (see Figure 4.4 and Figure 4.5). In agreement with previous observations, increased engine load results in decreased cycle-to-cycle variations for the same injection timing. It is considered that the in-cylinder temperature during the compressions stroke increases with increased engine load, reducing the energy loss from fuel vaporization. It is also believed that more advanced injection timings allow for more complete vaporization of the fuel and better air-fuel mixing, resulting in greater combustion stability relative to lower engine load and later injection timing cases.

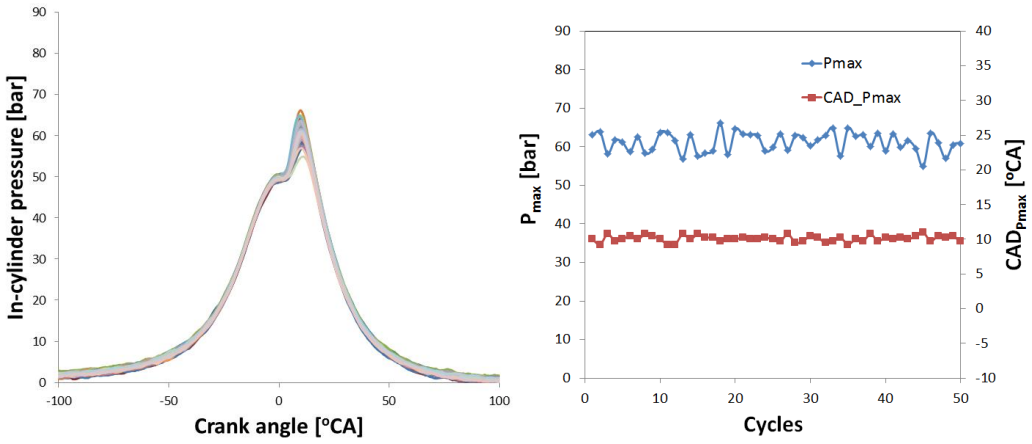

(a) BMEP=0.14 MPa

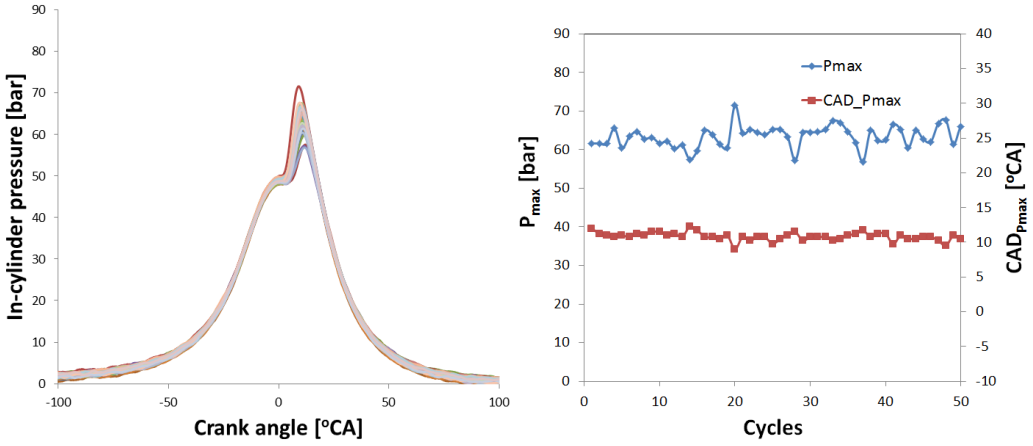

(b) BMEP=0.21 MPa

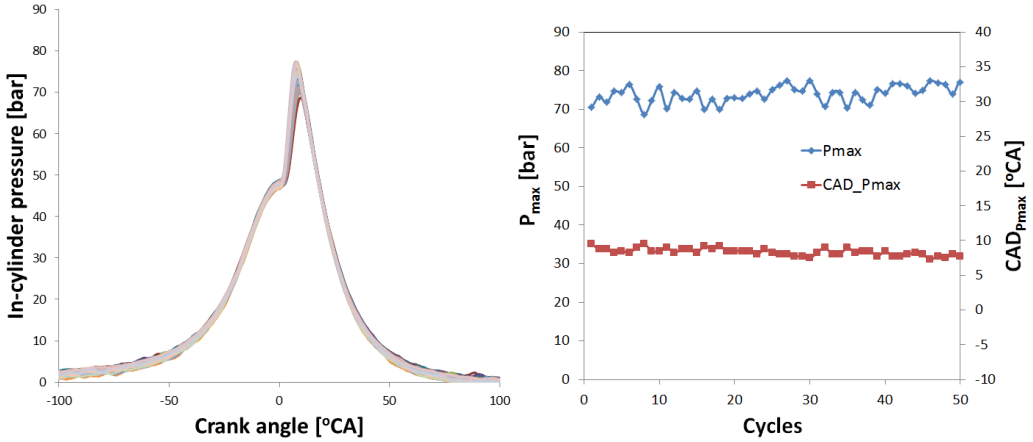

(c) BMEP=0.28 MPa

Figure 4.5 Cylinder pressures for multiple firing cycles and the histories of P_{max} and CAD_{Pmax} for 40%DME-60%NH_3, SOI=180 BTDC

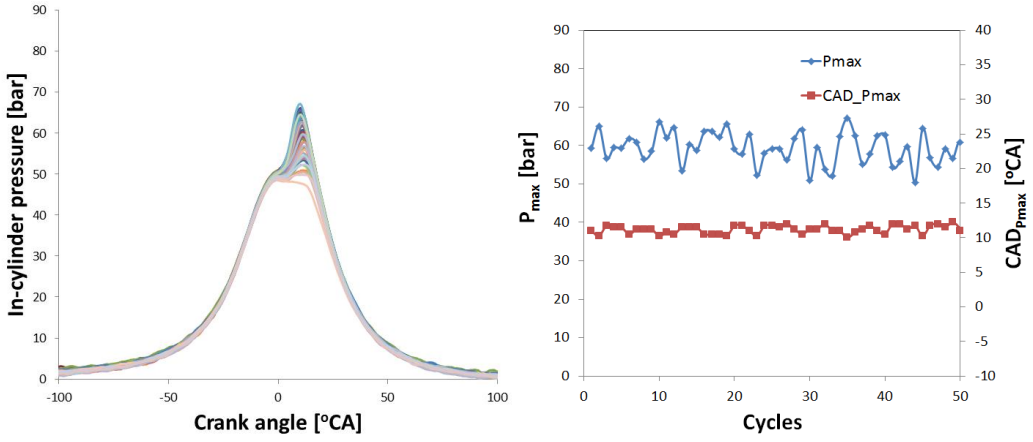

(a) BMEP=0.14 MPa

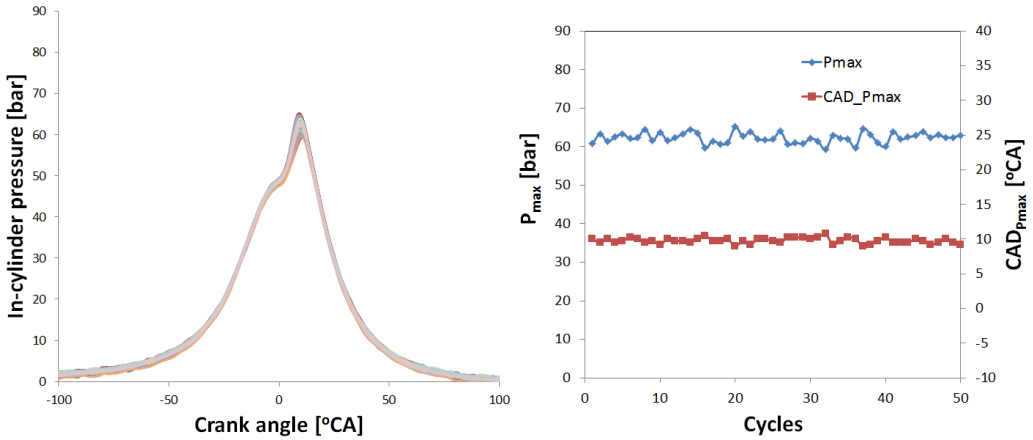

(b) BMEP=0.21 MPa

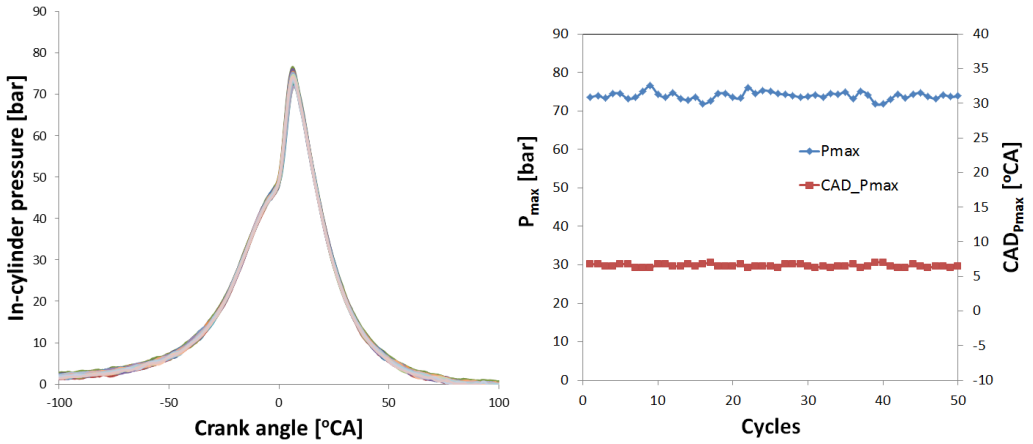

(c) BMEP=0.26 MPa

Figure 4.6 Cylinder pressures for multiple firing cycles and the histories of P_{max} and CAD_{Pmax} for 40%DME-60%NH_3, SOI=330 BTDC

A summary of combustion stability on ammonia-DME mixtures is presented in Figure 4.7 for representative injection timing for each fuel mixture. Note that the in-cylinder pressure data of 250 cycles are used to analyze the cycle-to-cycle variations presented in Figure 4.7. As can be seen, the inclusion of ammonia causes an increase in COV_{Pmax} and $COV_{CADPmax}$. The COV_{Pmax} and $COV_{CADPmax}$ for 100%DME are low,

approximately 1% and 0.11%, respectively. However, the COV_{Pmax} and $COV_{CADPmax}$ of 60%DME-40%NH_3 increase up to approximately 8% and 0.44% at high engine loads, respectively. A possible explanation for the higher fluctuation is attributed to the greater temperature loss due to more amount of ammonia supplied at higher loads, resulting in longer ignition delay and inducing more variability.

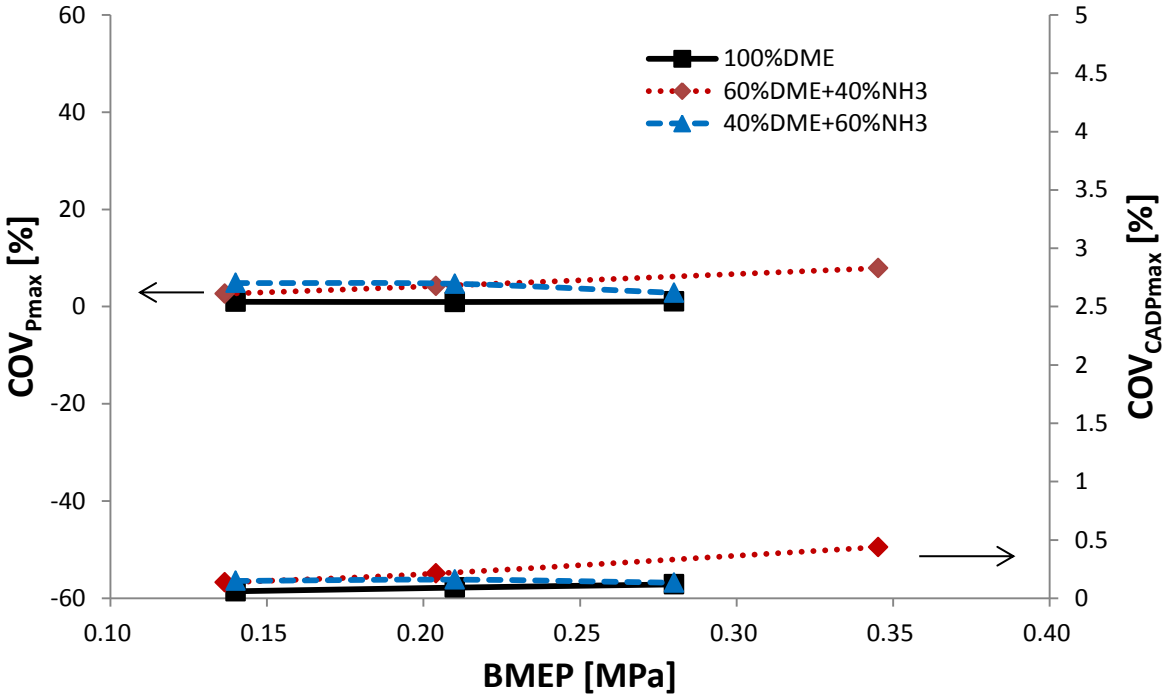

Figure 4.7 The coefficient of variation of peak pressure and the coefficient of variation of CAD_{Pmax} for various fuel mixtures

Meanwhile, for 40%DME-60%NH_3 the combustion is reasonably stable compared to 60%DME-40%NH_3, but COV_{Pmax} and $COV_{CADPmax}$ is still higher (~ 5% and 0.16%) than those for 100%DME. These results are consistent with those of HCCI engines. This can be a result of incomplete combustion during some cycles, which would dramatically increase HC and CO emissions. It is also believed that the evaporation of ammonia will

lower the in-cylinder temperature during the compression process, causing unstable combustion. The cycle-to-cycle variation of 40%DME-60%NH_3 decreases gradually with increase of engine load. It is believed that when engine load is increased, the engine is able to reach stable combustion due to the increase of in-cylinder temperature.

Figure 4.8 shows the comparison of cylinder pressure and heat release rate data for selected cases that are representative of the combustion characteristics in this study. The injection timings are 10, 20, and 180 BTDC for 100%DME, 60%DME-40%NH_3, and 40%DME-60%NH_3, respectively. It can be observed from Figure 4.8 that the cylinder pressure history of 40%DME-60%NH_3 is different from those of 100%DME and 60%DME-40%NH_3. The cylinder pressure of 40%DME-60%NH_3 is slightly higher during the compression process relative to the other cases even though the heat release rate indicates no combustion until after TDC. The pressure trace of 40%DME-60%NH_3 also exhibits a lower pressure than 100%DME and 60%DME-40%NH_3 during the expansion process. Detailed reasons will be explained later.

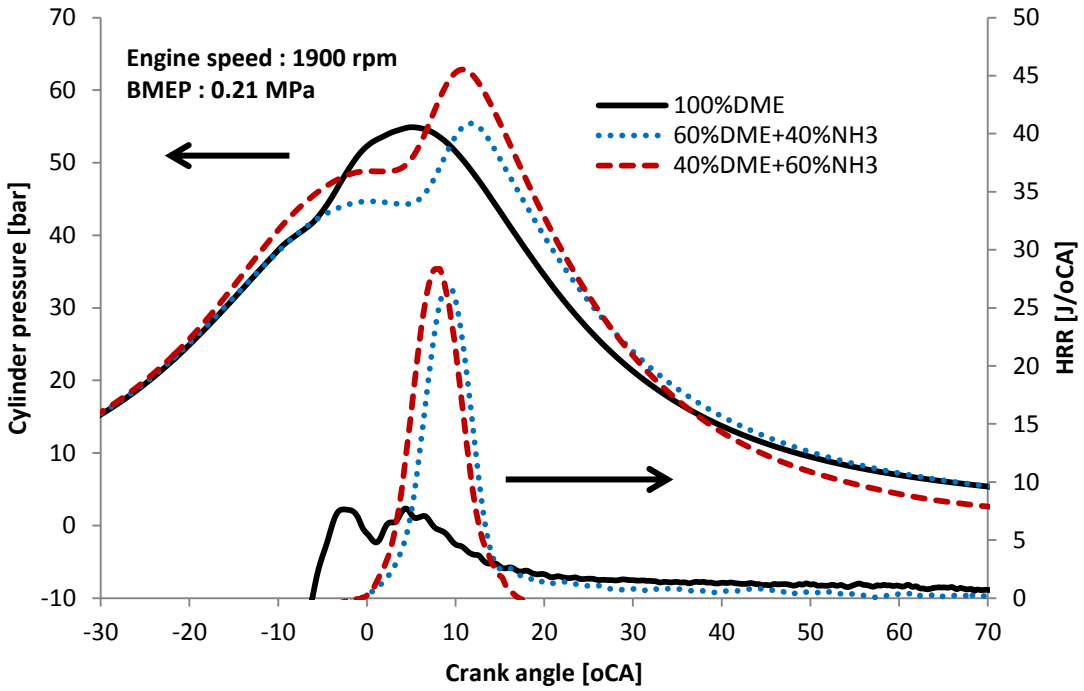

Figure 4.8 Cylinder pressure and heat release rate for various fuel mixtures

100%DME exhibits conventional diesel combustion with a premixed combustion phase, mixing-controlled combustion phase, and late combustion phase identified in the typical compression-ignition engine. The ignition delay is 4 crank angle degree (CAD) for 100%DME. For 60%DME-40%NH_3, a longer ignition delay (19.5 CAD) is observed, causing a very significant premixed combustion. The late combustion phase is also seen from the heat release rate data. Alternatively, with highly advanced injection timing, 40%DME-60%NH_3 has a homogeneous combustion phase with short combustion duration.

It is considered that the early injection of 40%DME-60%NH_3 causes complete evaporation of fuel during the intake and compression process. The rise of in-cylinder pressure prior to combustion is then attributed to the increase of vapor pressure in the

cylinder. The early injection also allows fuel and air sufficient time to fully mix, resulting in homogeneous combustion. 100%DME and 60%DME-40%NH_3 demonstrate typical diesel combustion and maintain higher in-cylinder pressure during the expansion process compared to the combustion of 40%DME-60%NH_3. The reduced pressure of 40%DME-60%NH_3 in the expansion stroke is a result of lower combustion temperature as seen from the exhaust temperature in Figure 4.12.

Figure 4.9 shows the cumulative heat release fraction (i.e., mass burn fraction) corresponding to the conditions in Figure 4.8. As can be seen from Figure 4.9, the combustion of 100%DME steadily advances through 140 ATDC, indicating slow diffusion combustion at the later stage. 60%DME-40%NH_3 has 90% heat release within 40^{o}CA after ignition and continues to release heat through 70 ATDC, exhibiting greater premixed combustion phase and smaller mixing controlled combustion phase, similar to premixed charge compression ignition. Unlike the two previous cases, the combustion duration of 40%DME-60%NH_3 is extremely short (20 CAD), which is a result of early fuel injection timing and exhibits HCCI combustion. These trends also appear in the high speed and high load conditions as shown in Figure 4.10.

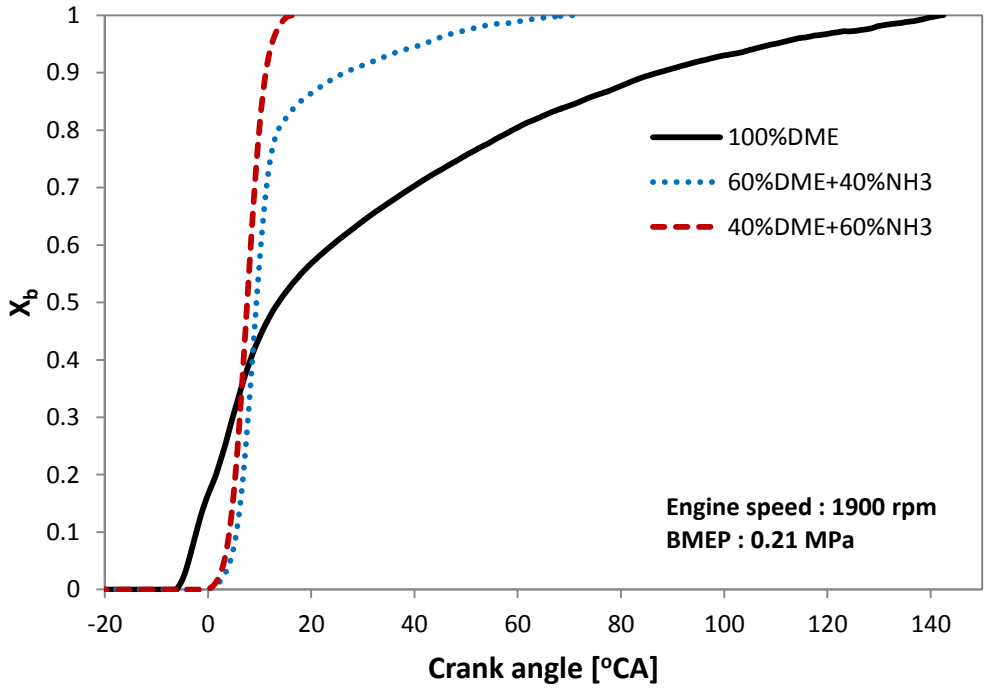

Figure 4.9 Mass burn fraction for various fuel mixtures

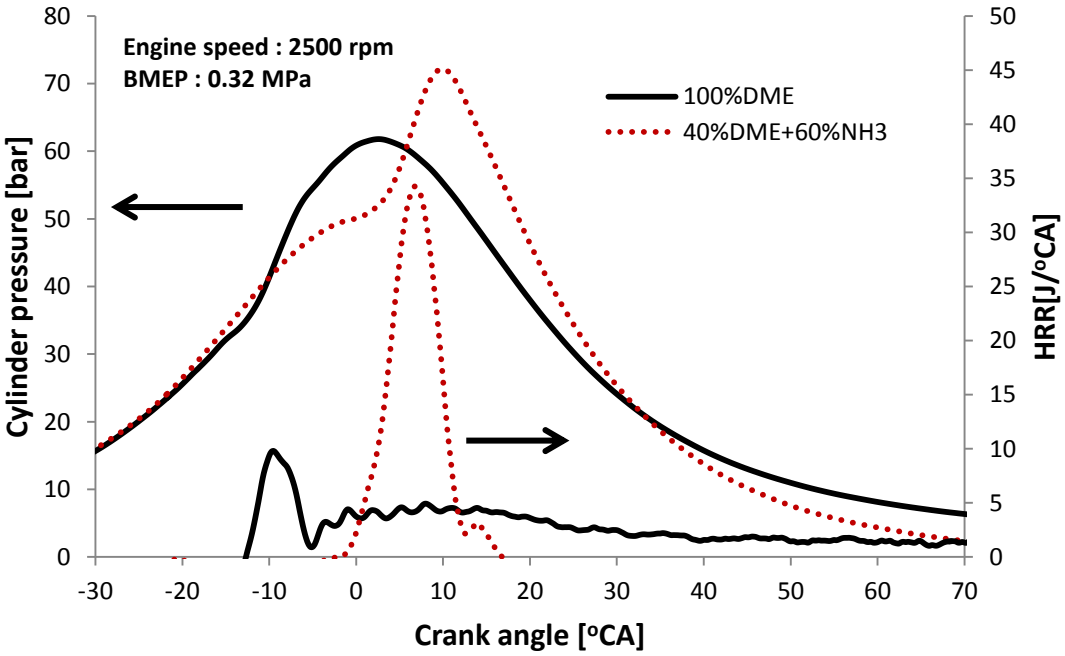

Figure 4.10 Cylinder pressure and heat release rate for various fuel mixtures

It is of interest to further investigate the combustion characteristics using high concentration of ammonia. The peaks of in-cylinder pressure and heat release rate increase with increased engine load for 40%DME-60%NH_3 as shown in Figure 4.11(a). It is believed that the increase of the engine load increases the in-cylinder pressure and temperature, mitigating the effects of high latent heat and resulting in more complete combustion and shorter combustion duration. It is seen from Figure 4.11(b) that as the fuel injection timing is advanced, combustion occurs earlier in the cycle, resulting in a higher peak pressure. Advanced timing also leads to short combustion duration. The advanced injection timing also allows more time for the fuel to evaporate and thoroughly mix with air, resulting in HCCI characteristics.

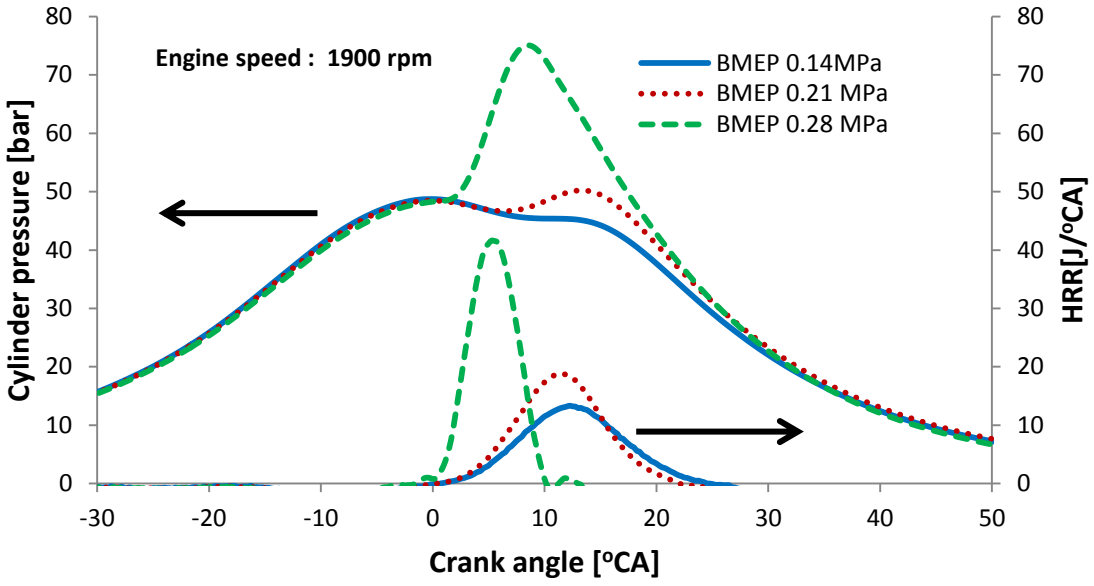

(a) Effect of engine load (SOI=160 BTDC)

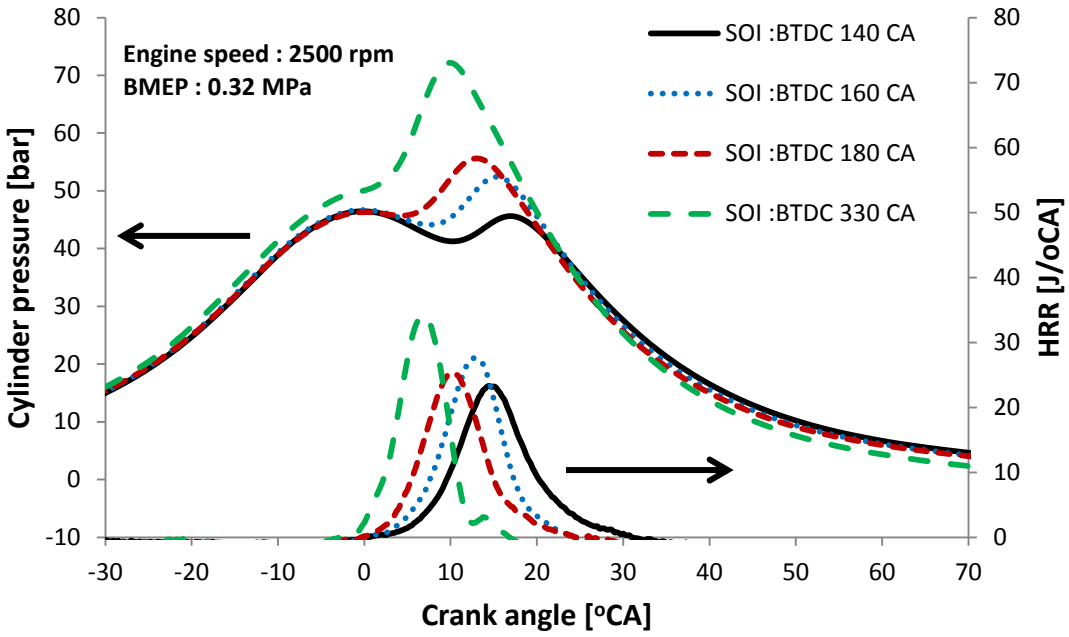

(b) Effect of fuel injection timing

Figure 4.11 Cylinder pressure and heat release rate for 40%DME-60%NH_3

Figure 4.12 shows the comparison of exhaust temperature versus break mean effective pressure (BMEP). The exhaust temperatures for 100%DME are higher than those for both 60%DME-40%NH_3 and 40%DME-60%NH_3. It should also be noted that as the ammonia concentration in the fuel is increased, the exhaust temperature decreases. The reduction in exhaust temperature is due to the loss in energy of the combustion process caused by the high latent heat of ammonia. This is especially evident in the case of 40%DME-60%NH_3 where the fuel charge has had sufficient time to fully evaporate, drawing the full latent heat energy out of the in-cylinder air.

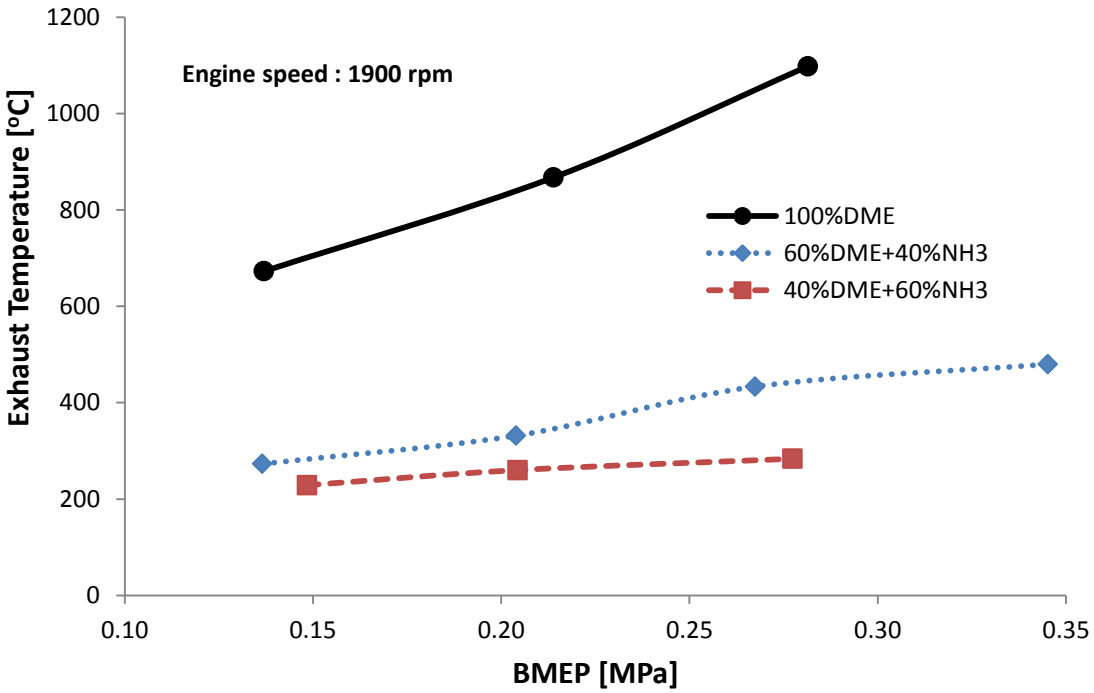

Figure 4.12 Exhaust temperature for various fuel mixtures

4.1.3 Soot Emissions

Emissions are presented in terms of brake specific emissions in this study. Figure 4.13 shows soot emissions for the three fuel mixtures. It is found that soot emissions for 60%DME-40%NH_3 and 40%DME-60%NH_3 are slightly greater than those for 100%DME; however, all three fuel mixture exhibit very low soot levels of which do not exceed 0.002 g/kWh. It should be noted that both fuel mixtures containing ammonia produce higher levels of soot than 100%DME even though the mixtures containing ammonia have fewer carbon. This can be attributed to the higher levels of incomplete combustion present in the 60%DME-40%NH_3 and 40%DME-60%NH_3.

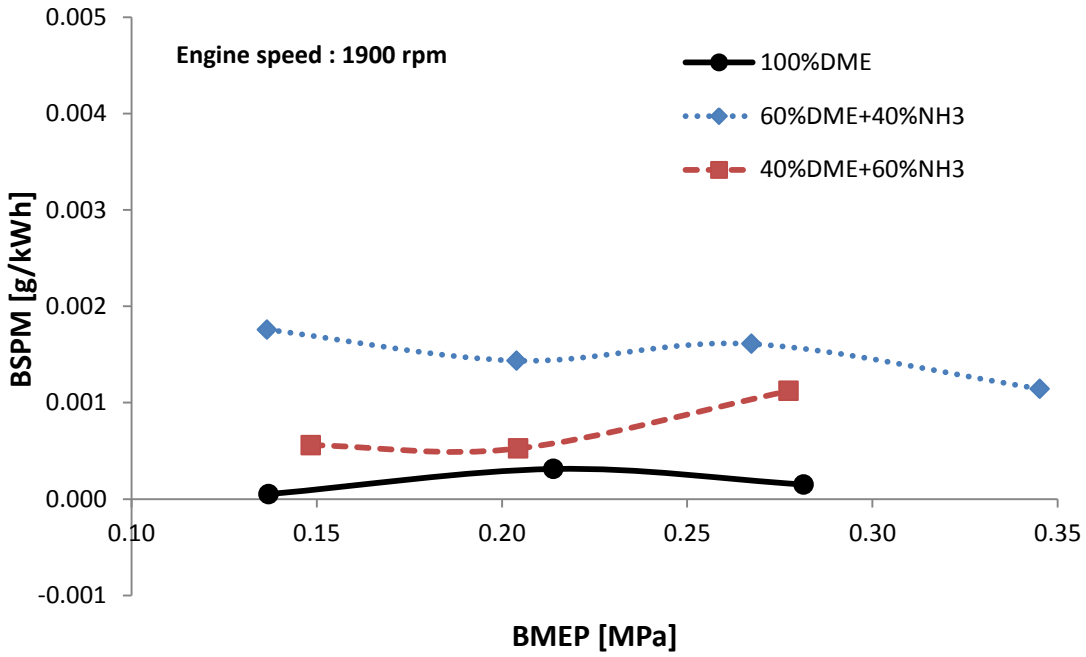

Figure 4.13 BSPM for various fuel mixtures

4.1.4 NO_x and NH_3 Emissions

Figure 4.14 shows NOx emissions for different fuel mixtures versus BMEP. It is found that NOx emissions for ammonia mixtures increase considerably relative to 100%DME, but still do not exceed EPA emission regulations (7.5 g/kWh) for small output engines [10]. The level of NOx emissions is approximately 6.5 g/kWh for 40%DME-60%NH_3 at 1900 rpm. It is believed that the increase in NOx emissions is primarily due to fuel NOx formation generated from ammonia combustion.

Ammonia emissions are shown in Figure 4.15. One of the concerns of using ammonia for combustion is the exhaust ammonia emissions, which can be toxic. As ammonia in the fuel mixture is increased, emissions increase significantly for low loads. For 40%DME-60%NH_3, ammonia emissions are approximately 16 g/kWh at low load conditions. However, as load is increased, ammonia slip is reduced to 11.4 g/kWh and

6.4 g/kWh for medium load and high load, respectively. Although a reduction in ammonia slip is observed at high loads, the exhaust still contains approximately 1,000 ppm of ammonia. At these levels ammonia is extremely hazardous, and thus appropriate exhaust after-treatment is needed, e.g., ammonia scrub by water bath or selective catalytic reduction (SCR). It may be possible to implement a process similar to those used in SCR systems to convert exhaust ammonia and NOx simultaneously. In the present ammonia engine scenario, since ammonia is present in the exhaust, it may be used directly without urea injection.

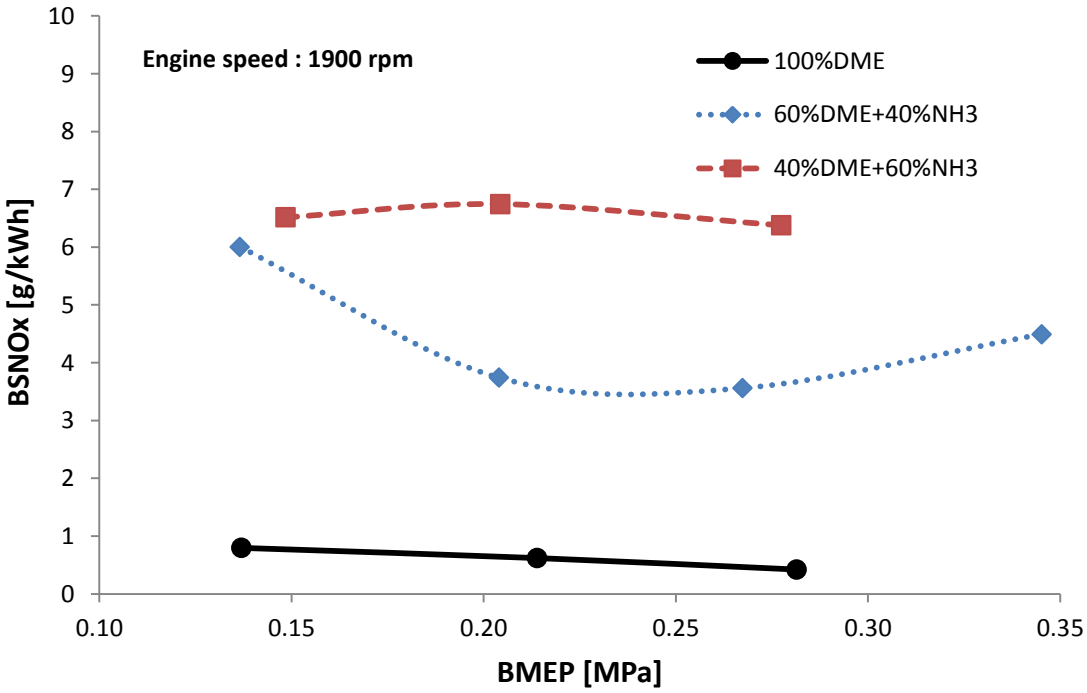

Figure 4.14 BSNOx for various fuel mixtures

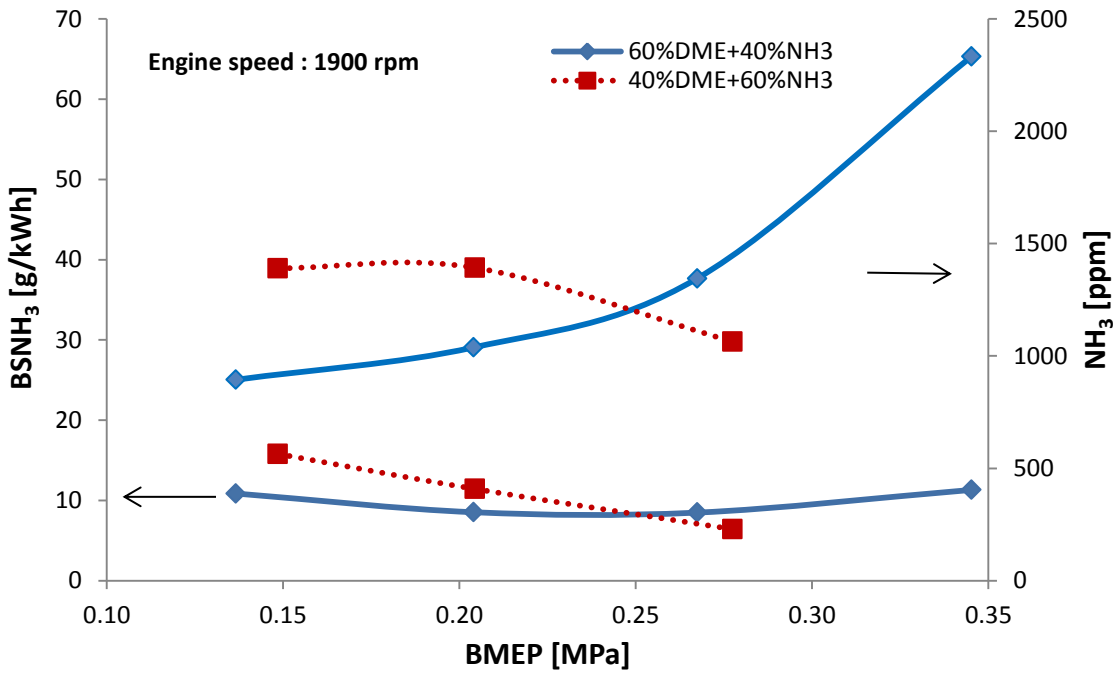

Figure 4.15 NH_3 exhaust emissions for various fuel mixtures

4.1.5 CO and HC Emissions

Figure 4.16 and Figure 4.17 show the emissions of unburned hydrocarbons and carbon monoxide for all three fuel mixtures. The EPA emissions regulations for HC and CO for small output CI engines are 7.5 g/kWh and 8.0 g/kWh, respectively [10]. The overall HC emissions levels using 60%DME-40%NH_3 are similar to those using 100% DME, whereas the HC for 40%DME-60%NH_3 is higher due to earlier injection timing, which causes lean, homogeneous, low-temperature combustion, leading to an increase in incomplete combustion. It is noted that unburned hydrocarbon emissions can be improved for higher BMEP using 40%DME-60%NH_3, which is attributed to an increase in in-cylinder pressure and temperature, thus resulting in more complete combustion. The CO emissions are also relatively high for all fuel mixtures. CO emissions for 100%DME, 60%DME-40%NH_3, and 40%DME-60%NH_3 at low load conditions are 10 g/kWh, 30

g/kWh, and 90 g/kWh, respectively. For both 100%DME and 60%DME-40%NH_3, CO emissions generally tend to increase with increased load, whereas CO emissions for 40%DME-60%NH_3 dramatically decrease with increased load. This can also be explained by significant incomplete combustion at low loads for high concentrations of ammonia.

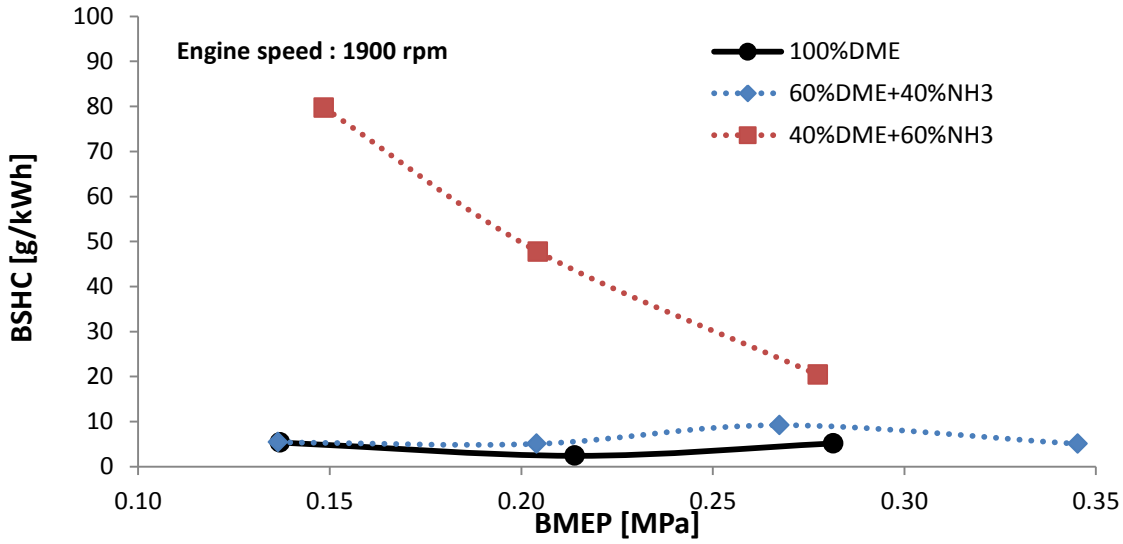

Figure 4.16 BSHC for various fuel mixtures

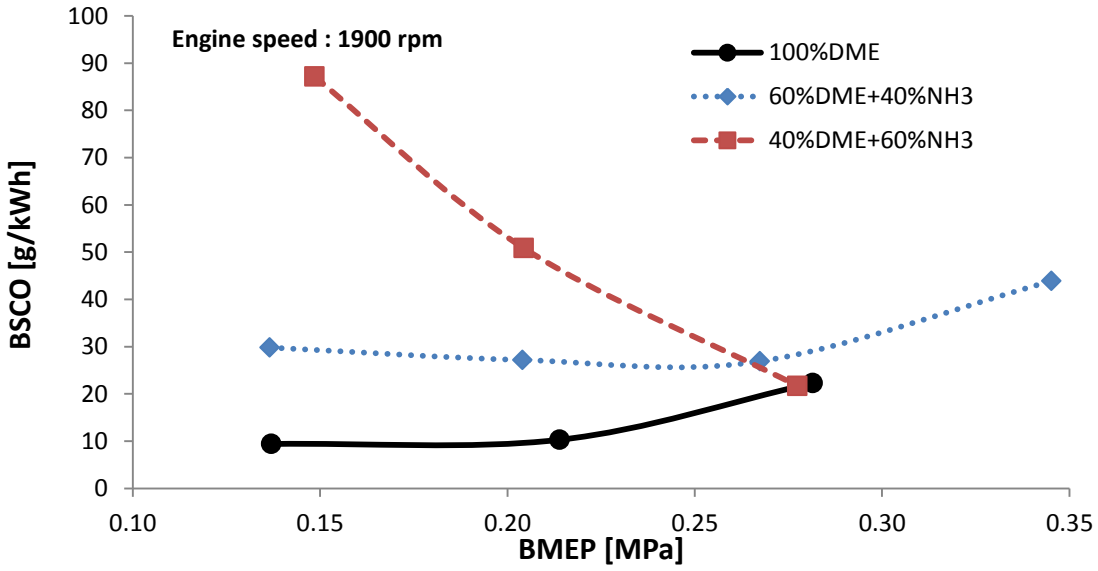

Figure 4.17 BSCO for various fuel mixtures

4.2 Gaseous Ammonia Direct Injection for SI Engine Application

Tests were conducted to determine the optimum injection timing and duration. During the test, gasoline was injected into the intake manifold with the injection pressure of 82 bar at the injection timing of 30 deg BTDC. The amount of gasoline injected was varied according to the base power. Tests were performed in two stages. First, it was concluded that in order to see appreciable increase in engine load from ammonia, injection timings had to be earlier than 270 BTDC. Thus, three injection timings were used, which included 270, 320, and 370 BTDC. For each injection timing, five injection durations were tested (10, 14, 18, 22, and 26 ms). Injection duration was measured in milliseconds (ms). In the second stage, based on the results from the previously described tests, five performance modes were determined based on power output, injection timing, and injection duration. Results of the engine performance, in-cylinder pressure history, heat release rate data, and emissions are detailed as follows.

4.2.1 Performance Characteristics

The performance characteristics of the gasoline-ammonia operation on the CFR engine were highly affected by the engine throttling capabilities. Because the engine does not have a throttle, unlike a regular gasoline engine, the overall control of the inlet air flow is very limited. The engine design is based on producing engine knock at full throttle. Running at full throttle provides several challenges with regards to the scope of testing for this experiment. We were able to observe that even at positive load equaling zero the engine required a substantial amount of fuel to sustain combustion. This problem was amplified by the high friction level present in the CFR engine. This issue

most highly affected results such as the maximum percentage of ammonia possible to operate the engine with positive load. This is a result of the much higher fuel to air ratio for combustion of ammonia relative to gasoline (Table 2.1). Since the combustion of gasoline was necessary to ignite the ammonia, the lower limit of gasoline in air by volume could not be exceeded. This value was seen as the idle condition of engine operation. In other words, a significant amount of gasoline is still required for the idling conditions.

The performance results are discussed below including brake specific energy consumption (BSEC) and variation in engine load compared to changing injection duration and timing. First discussed is the effect of ammonia injection timing and duration on engine load (Figure 4.18 and Figure 4.19). The first case discussed is the idle case, where the gasoline contribution was just able to sustain combustion prior to the introduction of ammonia. It is seen in Figure 4.18 that as the injection timing is advanced there is an increase in flywheel power. This is especially evident between 270 BTDC and both 320 and 370 BTDC. It is thought that the earlier injection timings allow for a higher flow rate of fuel. This is partially due to cylinder pressure increase during the latter part of the injection event. This problem is exasperated by the delay of fuel delivery caused by extended fuel bath resulted from the injector location design. It is also thought that earlier injection timings serve to displace some inlet air, which then results in combustion at conditions closer to stoichiometric. This is seen in the exhaust emissions as an increase in NOx/kg-fuel, which implies higher combustion efficiency of ammonia. The exhaust emissions are discussed in more detail at a later point. The next

point of interest is that injection timings of 370 and 320 BTDC exhibit nearly identical results for the first three injection durations (10, 14, and 18). However, there is an appreciable difference in the power output for injection durations of 22 and 26. It is thought that this is a result of injection pressure being overcome by the cylinder pressure late in the injection event.

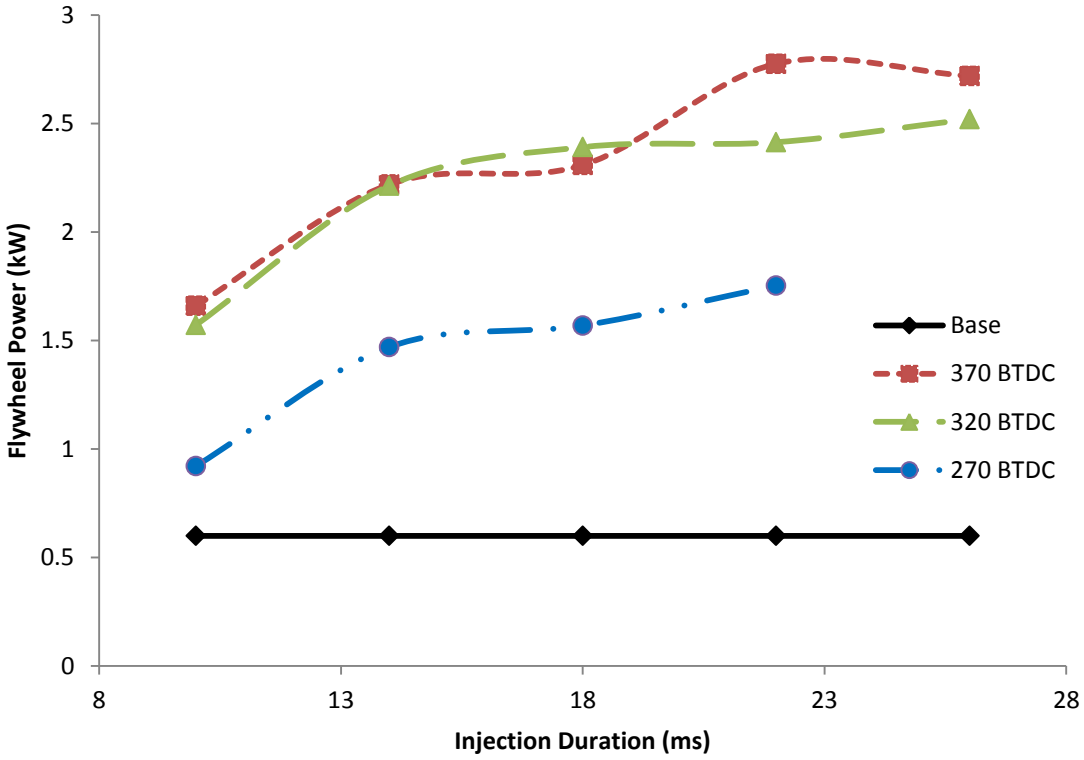

Figure 4.18 Flywheel power for varied injection timings for 0.6-kW baseline flywheel power

This general trend is seen for each increasing case of baseline gasoline levels (0.6, 1.4, and 2.3 kW) for the exception of the baseline of 3 kW, as seen in Figure 4.19. For this case the early injection timings (370 and 320) behave very similar, while the late injection timing of 270 outperforms both earlier ones. It is considered that the earlier

injection timings displace an excessive amount of inlet air, which results in highly rich fuel environment. The rich environment results in reduced combustion causing a decrease in engine flywheel power.

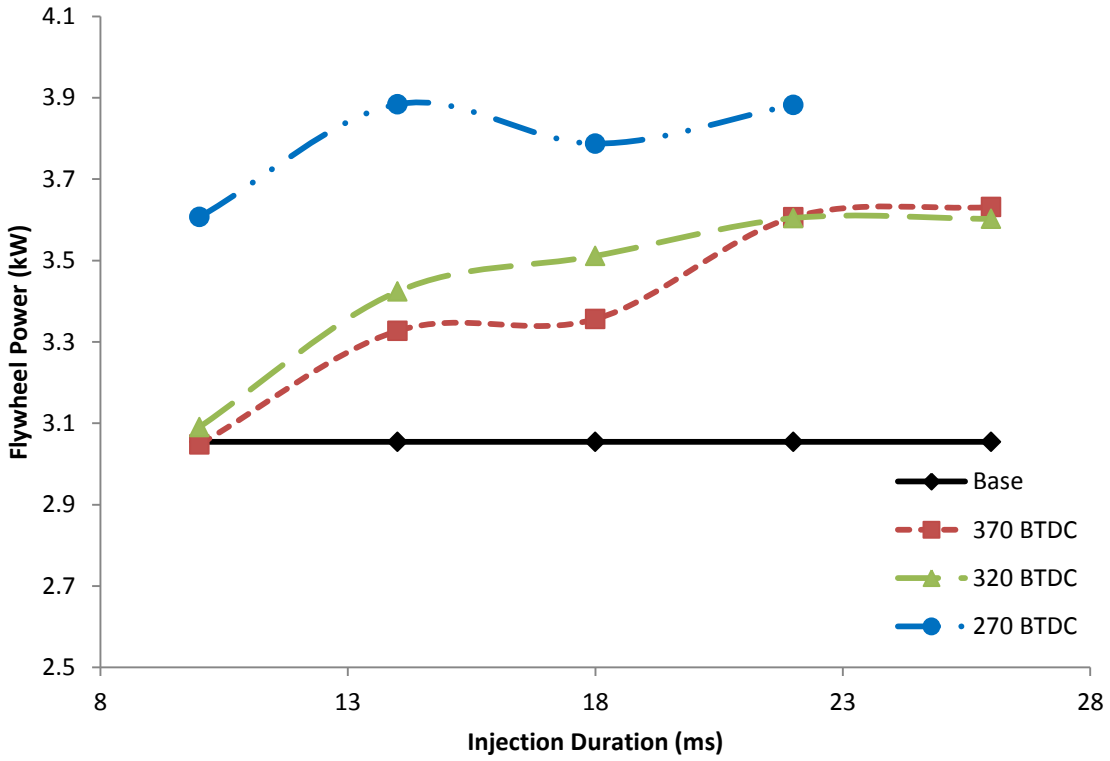

Figure 4.19 Flywheel power for varied injection timings for 3.0 baseline flywheel power

The compilation of all the gasoline baseline cases was used to develop a trend for potential contribution of ammonia with increased levels of gasoline as seen in Figure 4.20. It is clear from Figure 4.20 that as the initial amount of gasoline is increased the maximum power output contribution from ammonia is reduced. This is not expected from a direct injection system, where uniform contributions of ammonia across all initial gasoline levels are expected. There are two possible reasons for the decreased

contribution. First, at extremely early injection timings, the injected ammonia vapor displaces inlet air, resulting in a decreased volumetric efficiency and power output. Second, the engine is running on full throttle, which is a challenging issue for the present engine. Thus, there is simply not enough available oxygen in the system to support combustion and provide additional load at the higher gasoline levels.

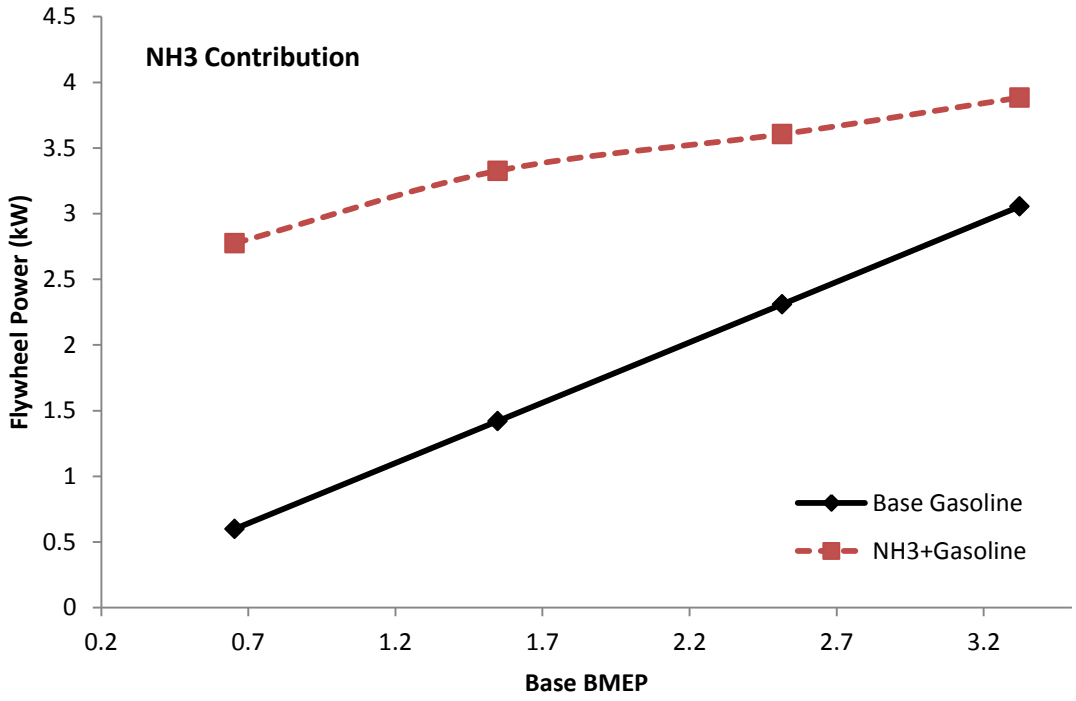

Figure 4.20 Contribution of full load from addition of ammonia

In further discussion the focus will shift to the performance modes as discussed earlier. Through testing and examining the effects of injection timing and duration, the optimal injection timing and duration were realized for set power outputs. By focusing on these performance modes it is possible to compare them to pure gasoline cases. The

results of those comparisons are discussed in further detail here. Two key factors are examined here. First is the BSEC for the ammonia performance modes and the gasoline performance modes as seen in Figure 4.21. BSEC was used in replace of brake specific fuel consumption (BSFC) because it was desirable to compare total energy usage as in BSEC rather than on a mass basis as in BSFC because the use of a dual fuel system. As seen in Figure 4.21 the BSEC for gasoline has little difference compared to the BSEC for gasoline-ammonia performance modes (see Table 3.5). This suggests that equivalent energy to gasoline was able to be provided by the ammonia over the range of loads.

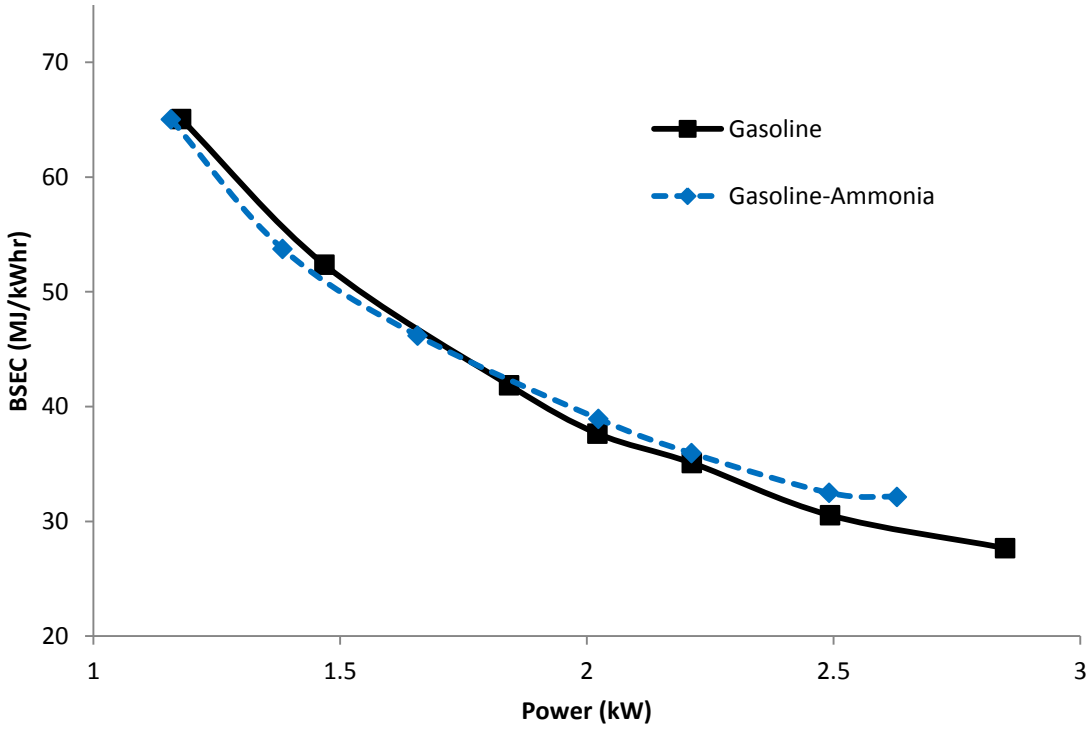

Figure 4.21 BSEC for gasoline and gasoline-ammonia

The exhaust temperature was of interest in this study because it acted counteractively to what may be considered typical. With the use of gasoline only, the exhaust temperature decreased with increased load. From examination of the HRR profiles it was noted that the combustion event decreased with increased load. Therefore, more energy of combustion was transferred into mechanical energy rather than exhausted in the form of heat.

4.2.2 Pressure and Heat Release Rate Histories

Comparing the pressure traces and HRR histories for ammonia performance and gasoline performance in Figure 4.22 and Figure 4.23, very similar curves are presented. Both follow the general convention of increased peak pressure with increased load with the exception of a few cases. HRR histories also follow similar trends with increased engine load resulting in a shorter more intense combustion event that occurs at a slightly earlier CAD. It is observed that the peak pressures for specific performance modes are slightly higher for gasoline. Reduced peak pressure signifies a reduction in combustion efficiency from gasoline-ammonia compared to gasoline. It is thought that the slow flame speed of ammonia increases the overall time of the combustion event, causing reduced thermal efficiency for the entire system. The peak pressure comparison for gasoline-ammonia and gasoline is demonstrated and discussed in more detail in the Catalyst Results section.

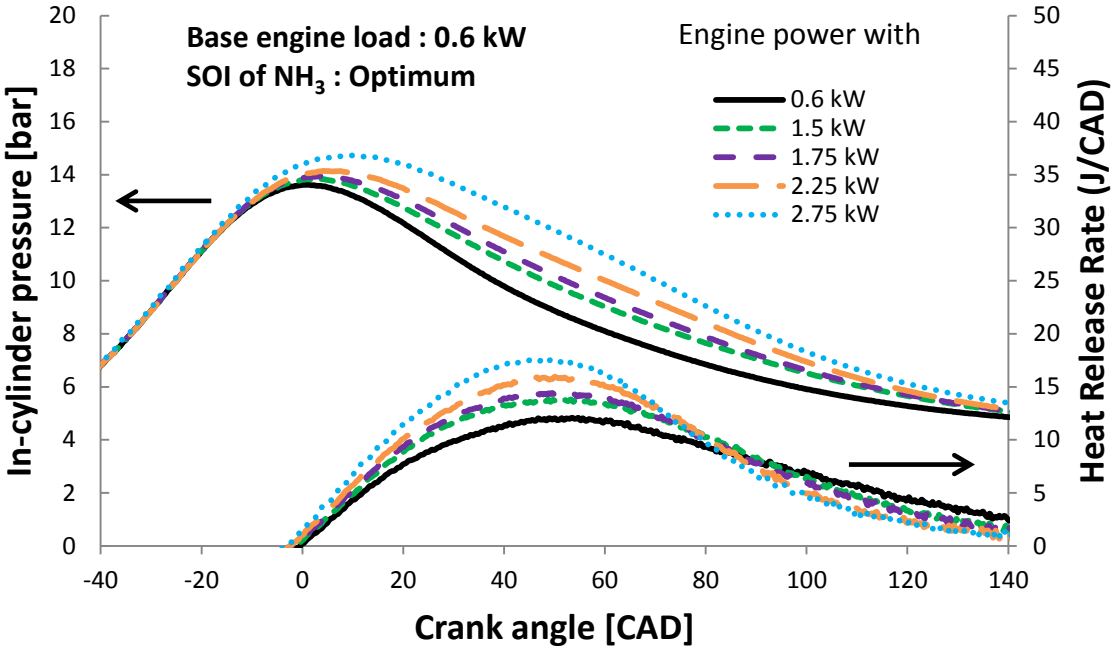

Figure 4.22 Pressure traces and HRR histories for performance modes using gasoline-ammonia

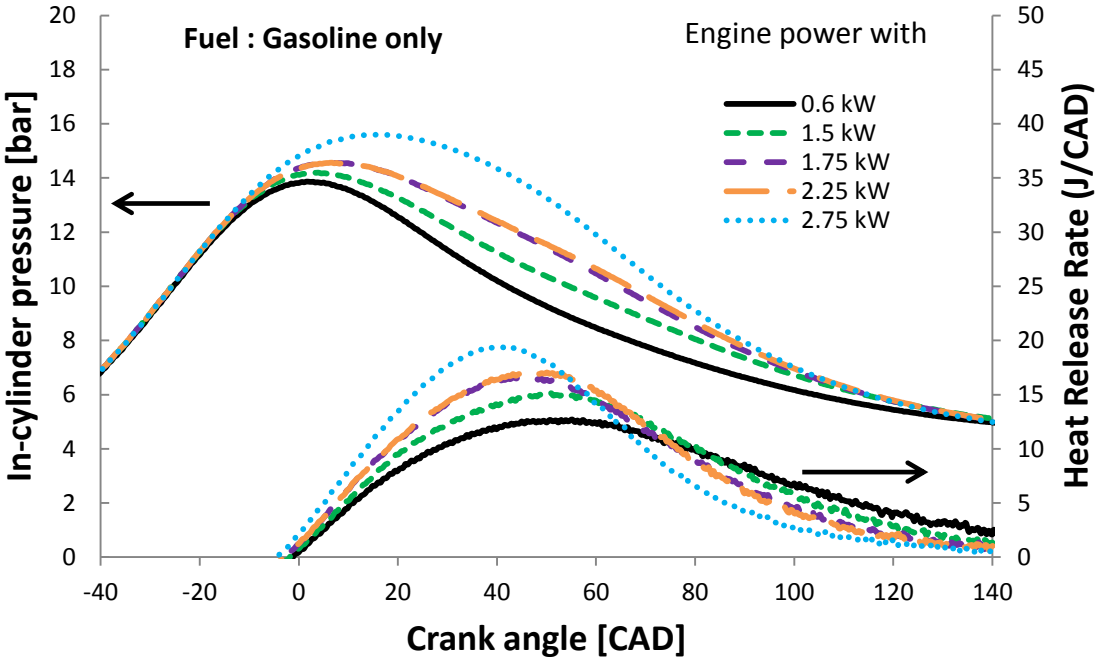

Figure 4.23 Pressure traces and HRR histories for performance modes using gasoline

Figure 4.24 shows the accumulative HRR for the gasoline-ammonia performance modes. It is seen that the general trend indicates that as the load is increased, the accumulative HRR also increases.

The normalized accumulative HRR in Figure 4.25 shows a decrease in duration of the combustion event with increased load. The important implications of decreased combustion time are that the addition of ammonia is not inhibiting combustion but rather increasing the combustion rate. This does not mean that ammonia increases the combustion rate to the extent that gasoline does, as has been noted the combustion event of gasoline performance is even less than that of ammonia. However, it does mean that the combustion of ammonia has a comparable event length to that of gasoline. It is considered that this is caused by the strong combustion due to the injection of ammonia into the cylinder chamber during the intake process, resulting in strong turbulence of the gasoline air mixture already present prior to spark event.

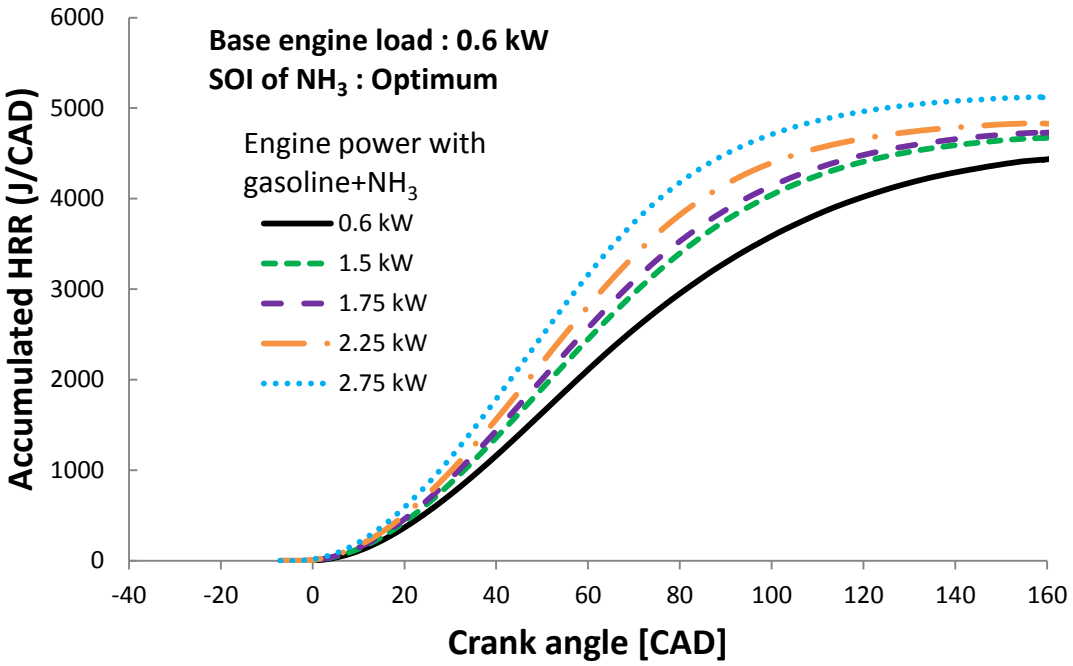

Figure 4.24 Accumulated HRR for performance using ammonia

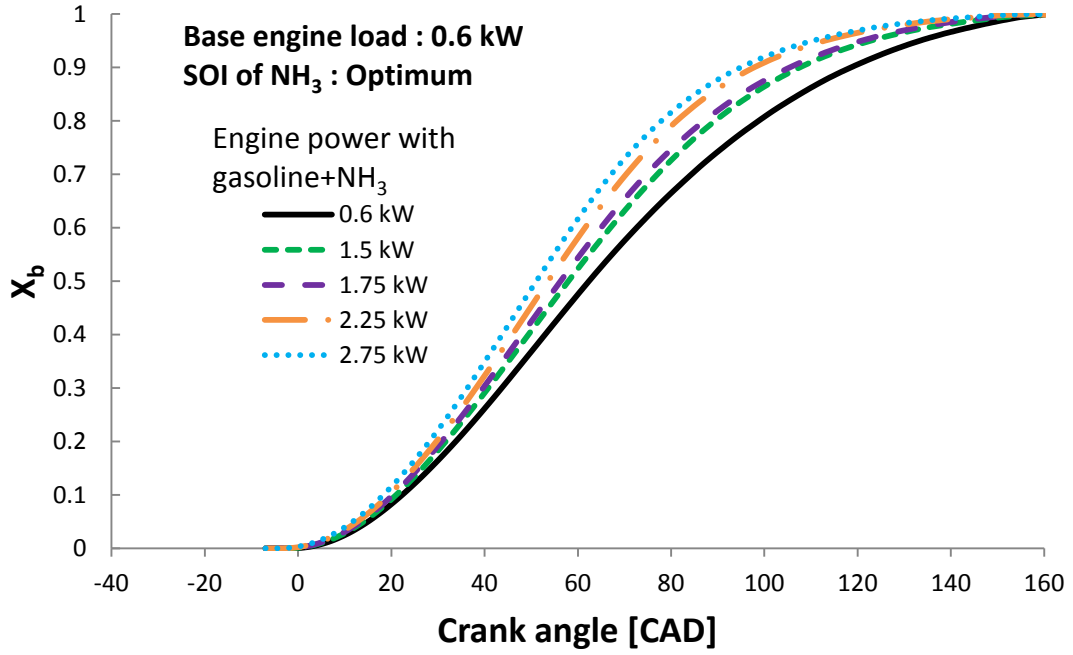

Figure 4.25 Fraction burned for performance modes using ammonia

4.2.3 NH_3 and NOx Emissions

Increased levels of ammonia injected into the combustion chamber results in both increased ammonia and NOx in the exhaust due to formation of fuel NOx and ammonia slip. Examining the ammonia and NOx emissions seen in Figure 4.26 it is evident that both tend to increase with increased power. The increasing NOx suggests increased combustion as NOx is primarily a result of fuel-bound nitrogen such as the nitrogen in ammonia. It is also seen that the ammonia levels in the exhaust also increase with increased load. This is a result of ammonia slip, where trace portions of the fuel are unburned and expelled in the exhaust. There two possible explanations for the increase of ammonia. The first is that with added ammonia comes reduced combustion efficiency. This is a distinct possibility as has been stated because of lower flame speed, increased minimum energy for ignition, and high latent heat of vaporization. However, combustion efficiency of ammonia does not reduce with increased load and remains at approximately 98% for all loads. Thus, it is concluded that ammonia slip in the exhaust is proportional to the amount ammonia injected as fuel. This then suggests that a relatively constant amount of fuel air mixture is allowed to slip into the exhaust unaltered in every cycle. This leads to the conclusion, that although there are increasing amounts of ammonia present in the exhaust with increased loads, it is not a result of diminishing combustion efficiency but rather a result of increasing amount of fuel ammonia. It should also be noted that the levels of ammonia present in the exhaust are relatively low and therefore there is inherent error in the measurements as read by the emissions analyzer. The error is used to explain the up and down fluctuations present

for ammonia. It is noted though that the general trend of increasing ammonia with increased load still holds true.

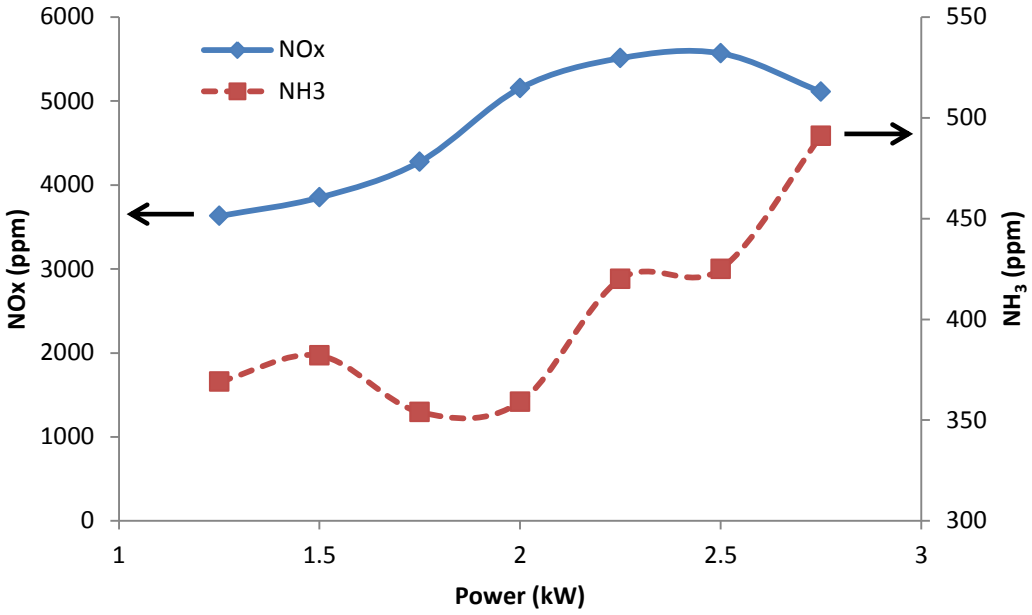

Figure 4.26 NOx and NH3 emissions for performance cases using gasoline-ammonia

Looking directly at parts per million (ppm) present in the exhaust of each substance says much less than comparing the power output and emissions as is done brake specific NOx or ammonia (BSNOx or $BSNH_3$). Figure 4.27 shows that both the BSNOx and $BSNH_3$ decrease with increased engine load. It is reaffirmed that the emissions efficiency with respect to both NOx formation and ammonia slip is increasing with increasing engine load. NOx is one concern of operating an ammonia powered engine. However, in cases where both ammonia and NOx are present it is possible to simultaneously reduce both using an SCR. With the use of an SCR slight ammonia slip

could be seen as a benefit as it would be used in the reduction of harmful NOx emissions.

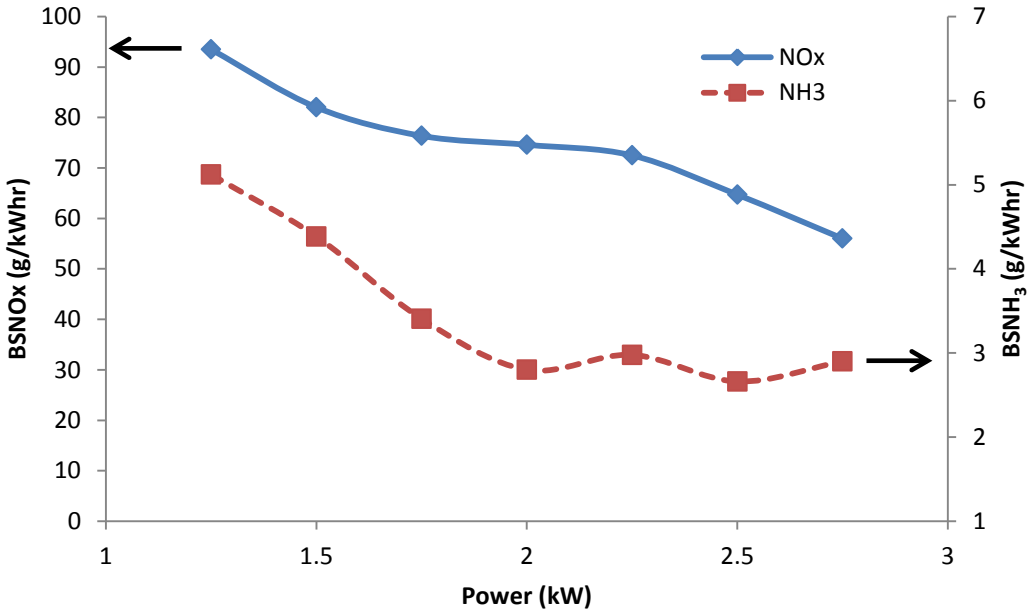

Figure 4.27 BSNOx and BSNH3 for performance modes using ammonia

It is important to compare emissions associated with the use of ammonia performance modes with those emissions present in gasoline performance modes. Figure 4.28 shows the BSNOx with respect to power for performance modes. The BSNOx for ammonia is significantly higher than that of gasoline. At this point it is necessary to discuss the extremely high level for BSNOx that is present for this experiment. It is believed that this is a combination of high temperatures (~800^{o}C) and fuel-bound nitrogen. It was observed that when using HCCI combustion techniques, even with 60% ammonia by mass in fuel there were very low NOx emissions. For the HCCI cases the exhaust temperature was also very low (~250^{o}C), which leads to the conclusion that the

much higher temperature present in the gaseous direct injection causes increased formation of fuel NOx. This conclusion is supported by $BSNH_3$ levels being similar to those seen in HCCI. An approach to reduce the NOx levels in the exhaust, beyond an SCR, would be to reduce combustion temperature.

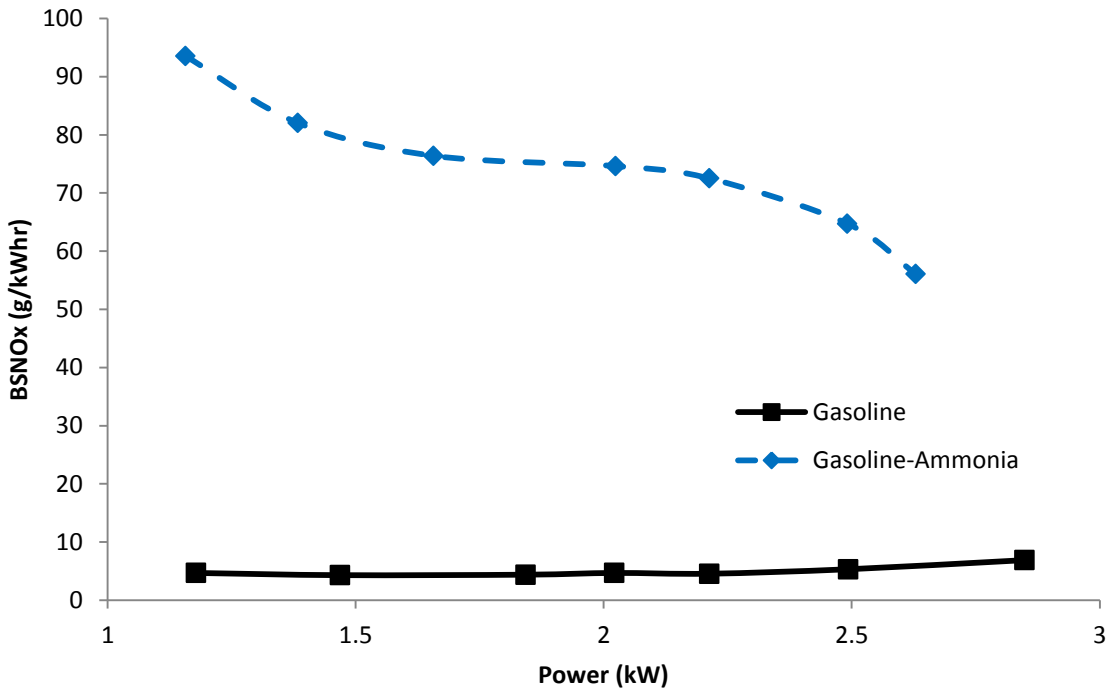

Figure 4.28 BSNOx for gasoline and gasoline-ammonia

4.2.4 CO_2, CO, and HC Emissions

As described one of the main goals of this research was limit the carbon emissions released during combustion of common petroleum based fuels. As ammonia has no carbon it is considered a fuel to help limit both CO and CO_2 emissions as well unburned fuel (HC). Carbon emissions data for performance modes are presented here. Examining

Figure 4.29 it appears ammonia has little effect on reducing CO_2 in the exhaust. However, it is important to consider one of the main challenges of using the CFR engine, which is the full throttle condition. Because of the full throttle condition the fuel required to achieve sustained combustion far exceeded the fuel required to move from the idle position to the high load condition. This is best illustrated by looking at the fuel flow of gasoline to achieve idle (sustained combustion-0.6kW) relative to achieving 2.75kW (high load condition), which were 27.5g/min and 30.9g/min, respectively. It is evident that although ammonia may reduce CO_2, it has little effect on the overall levels due to large fuel quantity needed to achieve idle. Evidence of slight improvements is seen in Figure 4.29 by the slight reduction of $BSCO_2$ in the gasoline-ammonia case. It is thought that with an engine capable of running at different throttle conditions, improvements of CO_2 emissions could be greatly advanced.

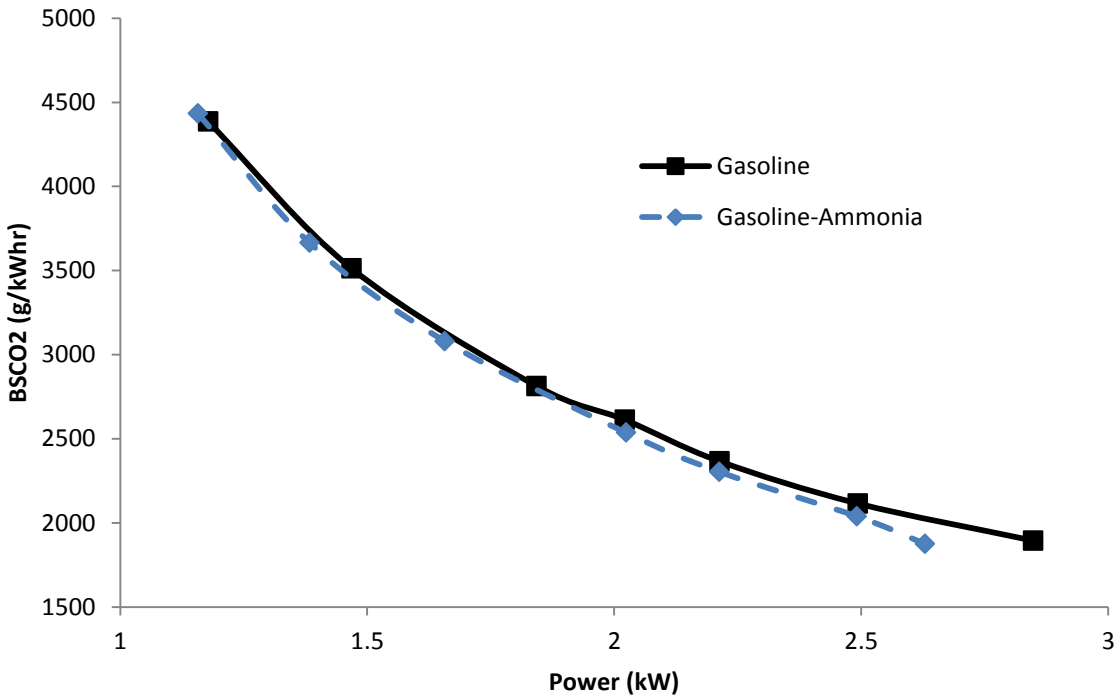

Figure 4.29 $BSCO_2$ for gasoline and gasoline-ammonia

Similar results are seen in Figure 4.30 for BSCO, although in this case both values are relatively low and well below the emissions standards for small SI engines of approximately 600 g/kWh [10]. Again the addition of ammonia causes slight reduction of BSCO for all presented loads. There are several possibly explanations for the reduction of CO. One possible explanation is that the ammonia is replacing the carbon fuel source. However, as it has already been noted due to the large amount of gasoline needed to achieve combustion the overall carbon emissions levels are affected little by the substitution of ammonia to produce excess power. Another possible explanation is that the combustion efficiency of the engine has been increased and the CO is being brought to complete combustion state of CO_2. This is reasonable because the little

addition to the CO_2 levels by conversion of CO would not change CO_2 levels due to the already high values. Examining Figure 4.31 presents an alternative option. As is seen in Figure 4.31 HC levels are increased with ammonia relative to gasoline. This then suggests that the introduction of ammonia is inhibiting combustion rather than propagating combustion. Less fuel is undergoing the combustion process, therefore, the partial product of CO is also reduced. This conclusion is also supported by the calculated combustion efficiencies, which were 99.3% and 99.6% for gasoline-ammonia and gasoline performance modes, respectively.

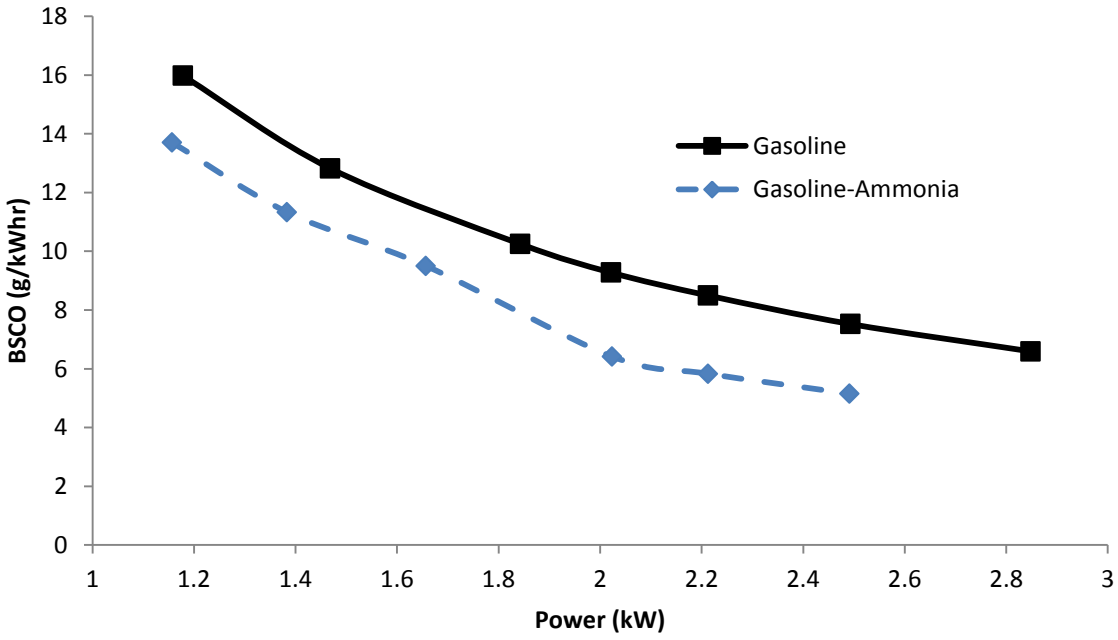

Figure 4.30 BSCO for gasoline and gasoline-ammonia

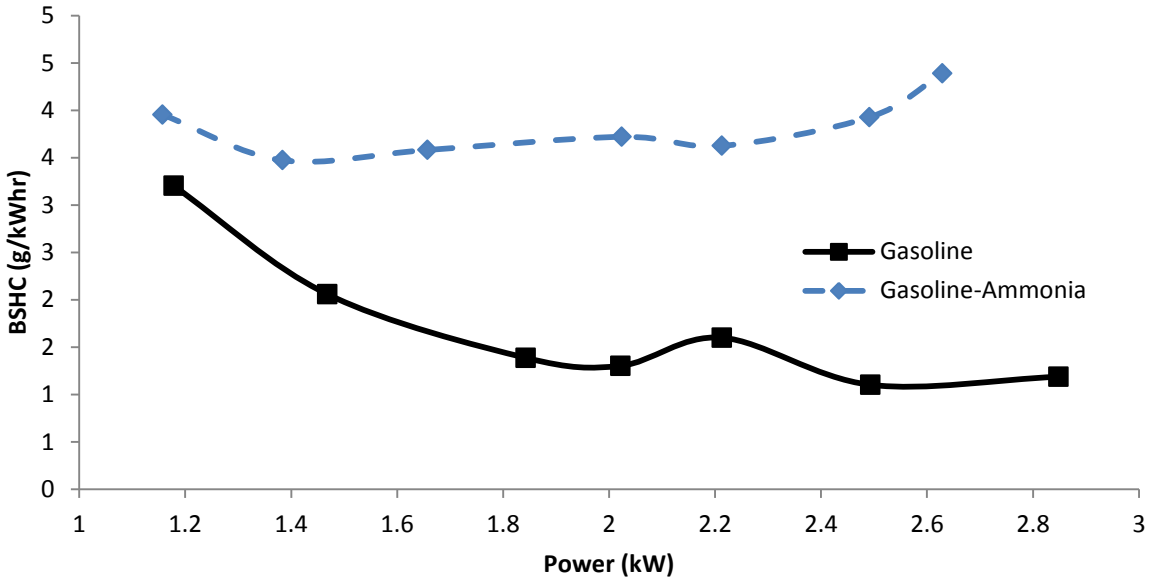

Figure 4.31 BSHC for gasoline and gasoline-ammonia

The results for carbon based emissions present little benefit from the use of ammonia over gasoline to produce positive power for the CFR engine. There were, however, several key factors that distort the results of the emissions analysis. The first and most important issue was the full throttle condition. The high level of gasoline fuel needed in order to achieve sustained combustion desensitized the emissions results to benefits that may have been attained by the use of ammonia. The second issue was the high combustion temperature of the engine which severely affected results such as NOx emissions. The combination of both these affects makes it difficult to ascertain measurable benefit for using ammonia with this particular engine configuration.

4.2.5 Catalyst Results

Emissions data with the addition of the ammonia dissociation catalyst are presented here in comparison with gasoline-ammonia and gasoline performance modes.

A measurable improvement of performance characteristics and exhaust emissions are experienced with addition of the catalyst. Improvements are especially apparent for low loads, which translates to low flow rate of ammonia through the catalyst. It is thought that greater catalyst surface area and longer exposure time would result in increased improvements for all load ranges. Justification for this conclusion will be discussed in detail with regards to Figure 4.32.

If the performance characteristics of the engine are examined both with and without the ammonia dissociation catalyst it is seen that with equal injection timing and duration the catalyst performs better than no catalyst (see Figure 4.32). It is observed that for short injection timings the case with a catalyst performs much better than the case without a catalyst. However, as the injection duration is increased both the catalyst and non-catalyst cases perform comparably. It is hypothesized that for low injection duration (low flow rate of ammonia) the catalyst is able to convert a high volume of the ammonia into hydrogen, resulting in improved combustion. As the injection duration is increased (increased flow rate) the catalyst is unable to maintain the same conversion rate, resulting in reduced performance. This is supported by the injection temperature of ammonia with catalyst present. It was observed that for short injection durations the injection temperature of ammonia was low (88^{o}C) while for longer injection duration the temperature was much higher (218^{o}C). It is thought that the lower temperature indicates that heat has been used in the dissociation reaction to decompose ammonia, while the higher temperature indicates that the heat used for ammonia dissociation is insignificant at high flow rates, probably because of the insufficient exposure or time for

ammonia decomposition to produce an appreciable amount of hydrogen in the mixture. It is then concluded that the catalyst was insufficient in the surface area and exposure time to achieve the desired conversion for all ranges of injection timing. It should be noted that although there are conversion charts for ammonia to hydrogen using dissociation catalysts based on temperature, in this experiment the temperature inside the catalyst chamber could not be measured. Therefore, the conversion rate can only be speculated based on the performance and emissions results.

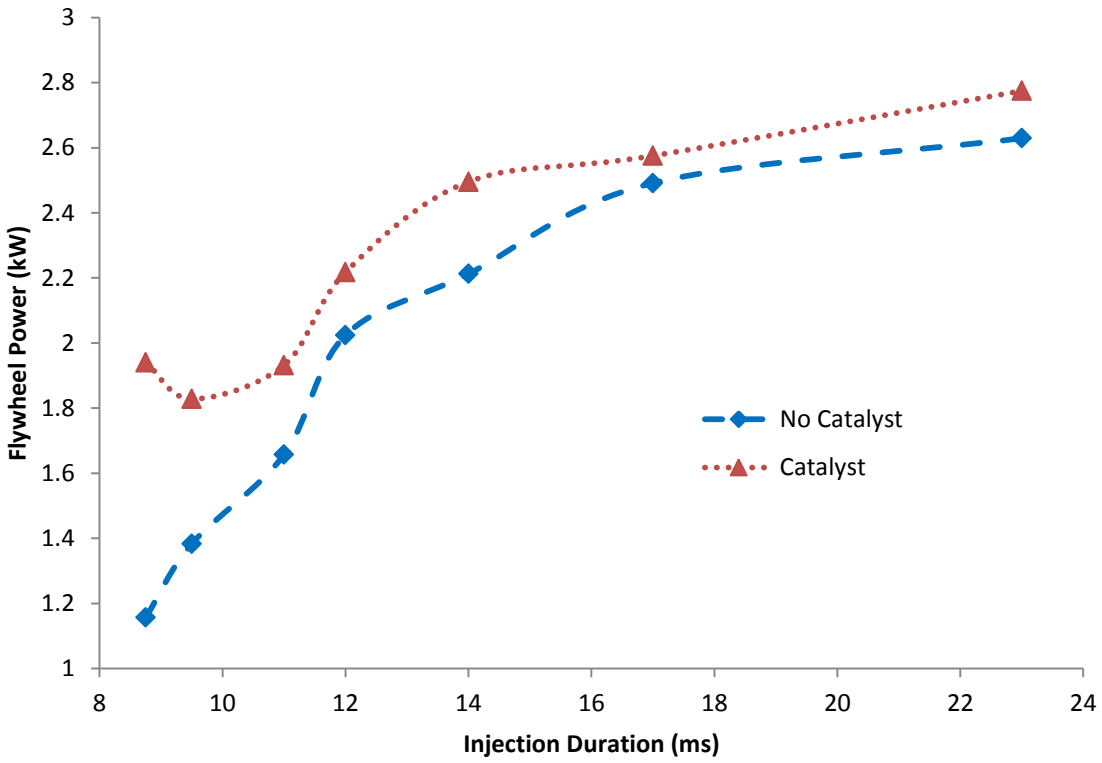

Figure 4.32 Flywheel power with and without a dissociation catalyst present

From the pressure history and HRR in Figure 4.33, it is observed that the catalyst performance modes act very typically for a gasoline SI engine. Increased load results in higher peak pressure. Ignition generally occurs at the same CAD for all cases and the

later end of the combustion characteristics exhibit the same curve for all loads. Looking at the HRR a slight advance in ignition and reduced time of combustion is seen with increasing load as well as a higher max HRR.

Of more noticeable interest is the pressure curve and HRR histories comparison of gasoline, ammonia, and catalyst performance modes as seen in Figure 4.34 and Figure 4.35. Comparisons are shown for 1.50kW and 2.75kW, which present an accurate representation of trends exhibited for all load conditions. The first observation is that gasoline exhibits a higher peak pressure as well as a higher peak HRR than ammonia. Early and late stages of the pressure and HRR curves exhibit very similar shape for gasoline and ammonia. It is thought that the slow flame speed of ammonia causes an elongated combustion event that result in lower peak pressure. It is seen that ammonia has a slight ignition advance over gasoline. This is thought to be a result of a richer fuel mixture of gasoline near the spark event. This phenomenon is thought to be caused by cylinder geometry combined with lower energy density of ammonia. The lower energy density of ammonia causes fuel-to-air ratio to be increased. The geometry of the cylinder is such that once the intake port is closed the continued injection of ammonia serves to push the gasoline air mixture closer to the spark source, thus, creating favorable ignition conditions near the spark source. It is also thought the injection of ammonia causes increased turbulence in the combustion chamber prior to the spark event resulting in an earlier ignition event.

With the addition of the catalyst several very interesting results are seen. The peak cylinder pressure for the catalyst is higher than the peak pressure for gasoline-

ammonia. Furthermore, the peak pressure of the catalyst exceeds that of gasoline as well. By examining the HRR histories a potential cause is identified. For not all loads is the peak HRR higher for the catalyst over gasoline as seen in the 2.75kW load case. As seen in the 1.5kW load case the peak HRR is higher for gasoline. However, in all cases it is observed that the combustion event is advanced by the use of the catalyst over both gasoline and gasoline-ammonia. The combustion event is generally short for the catalyst as well. It is thought that this is a result of two effects. First as was mentioned in discussion with regards to ammonia the cylinder geometry and lower energy density of ammonia play a role in advancing ignition. Then it is believed that with the addition of hydrogen there is a significant increase in flame speed, which results in an advanced and narrower combustion event. This advanced and narrow combustion event leads to a higher peak in cylinder pressure for the catalyst over both gasoline-ammonia and gasoline.

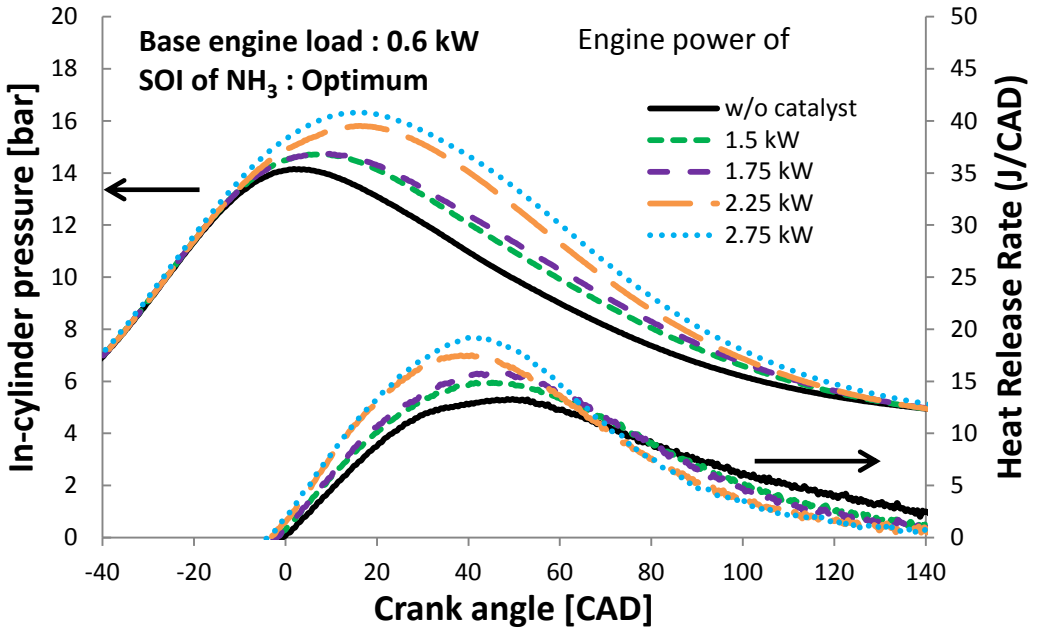

Figure 4.33 Pressure traces and HRR histories for performance modes using gasoline-ammonia with a catalyst

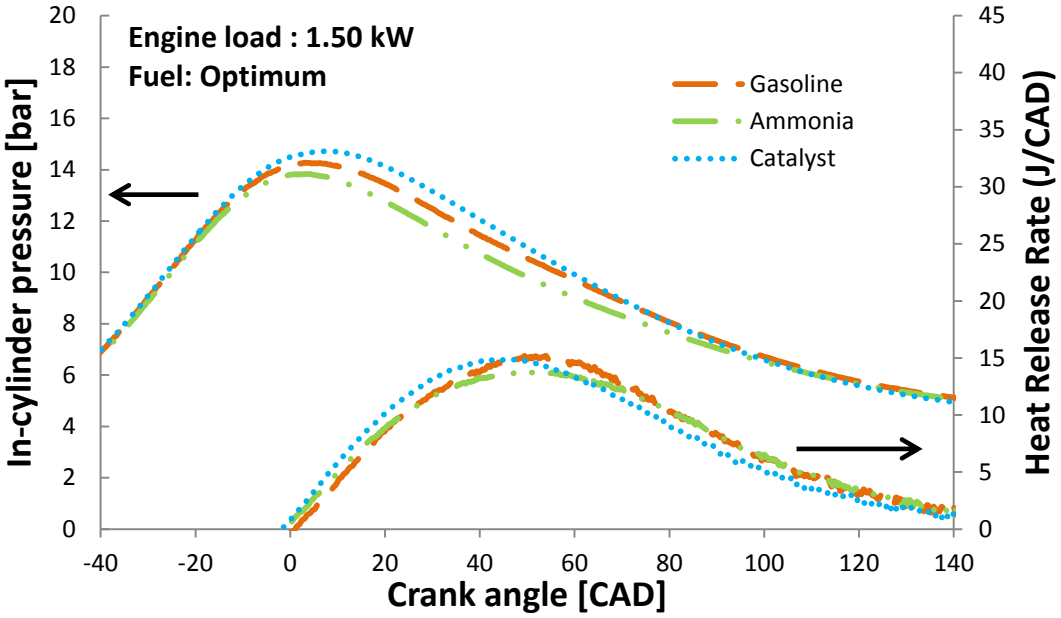

Figure 4.34 Pressure traces and HRR histories for various fuels at 1.50kW

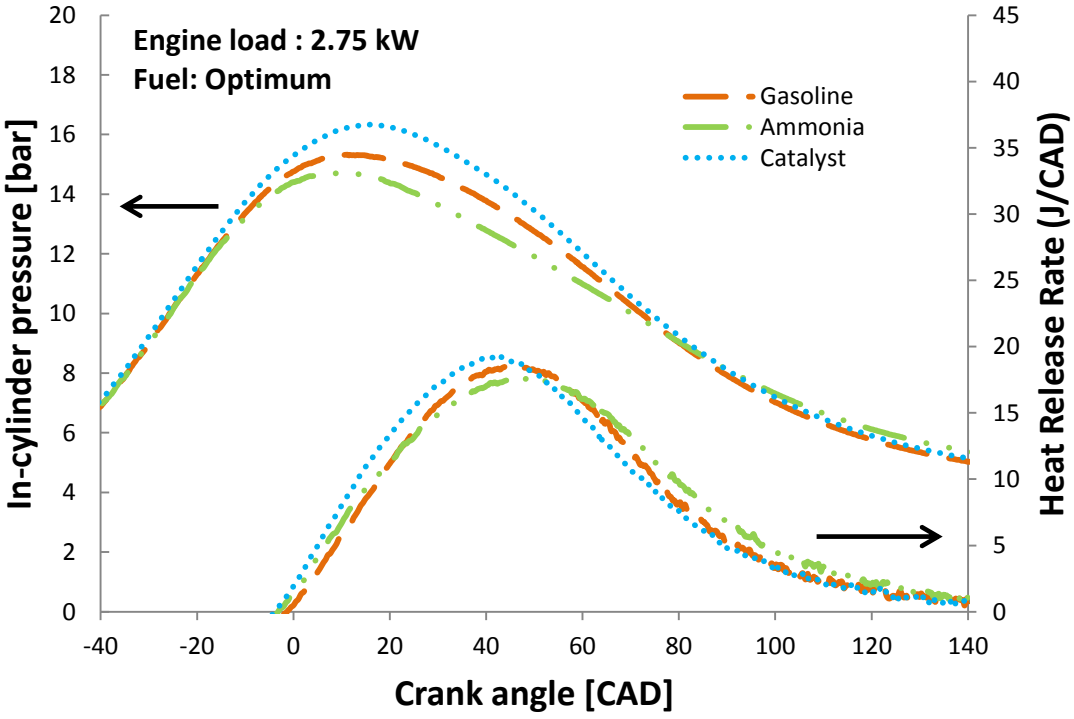

Figure 4.35 Pressure traces and HRR histories for various fuels at 2.75kW

Similar conclusions can be drawn from the comparison of BSNOx with and without the catalyst as was seen with the power output comparison. It is seen in Figure 4.36 that for short injection duration the BSNOx with the catalyst is significantly reduced but as the injection duration increases the BSNOx histories begin to converge. It is thought that as the ammonia is dissociated the free nitrogen is allowed to combine with other free nitrogen producing very stable N_2, thus reducing the fuel-bound nitrogen available for the combustion process. As discussed fuel NOx formation dominates NOx production and thus a reduction in fuel-bound nitrogen results in appreciable reduction in NOx production.

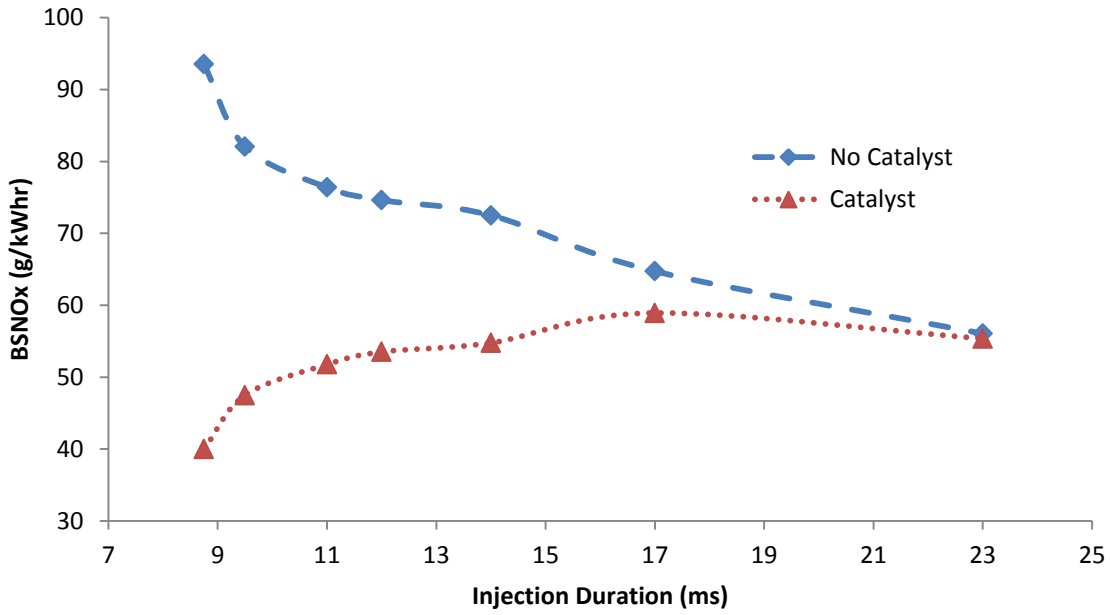

Figure 4.36 BSNOx with and without catalyst present

It is apparent from Figure 4.37 that the introduction of the catalyst and subsequent conversion of ammonia to hydrogen greatly increases the combustion efficiency. The $BSNH_3$ is reduced from 5 g/kWh to less than 1 g/kWh short injection durations and 3 g/kWh to less than 1 g/kWh for medium and long injection durations. The reduction of ammonia is a clear result of greater combustion efficiency and a reduced amount of ammonia per injection.

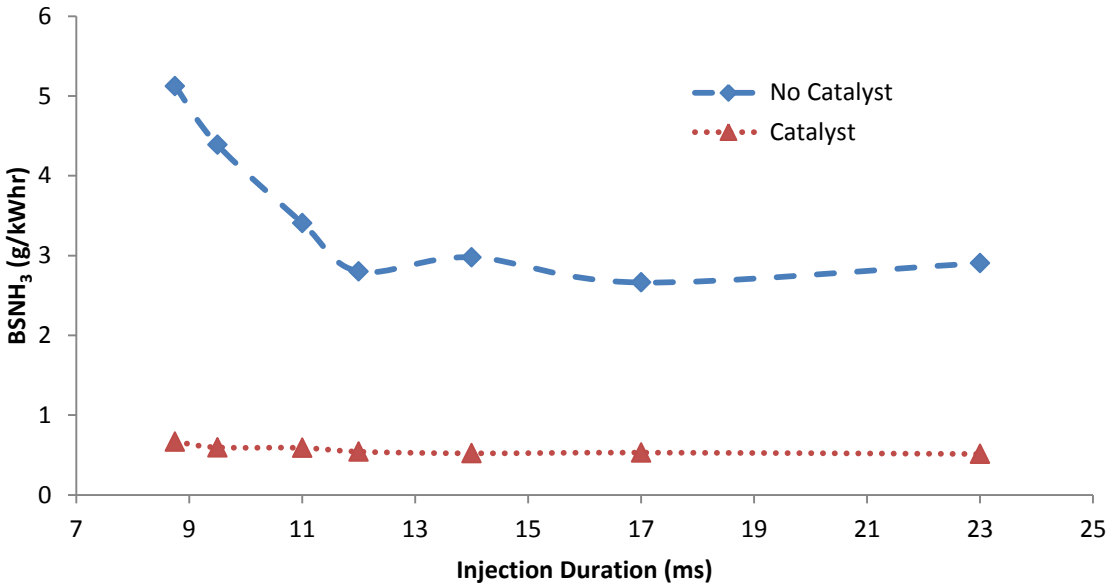

Figure 4.37 $BSNH_3$ with and without catalyst present

Figure 4.38 shows the BSCO for all performance modes. It is seen that the BSCO is further reduced by the addition of the catalyst. As was used to explain the reduction of CO with addition of ammonia it is possible to conclude that the addition of the catalyst further reduces the combustion efficiency resulting in increased levels of HC. However, as seen in Figure 4.39 the BSHC is actually reduced with the use of the catalyst to levels comparable with gasoline. Therefore, it must be concluded that the addition of the catalyst does increase the combustion efficiency, which simultaneously decreases CO and HC. Again it is observed that for both BSCO and BSHC the benefits of the catalyst diminish as the load is increased. This is thought to be a result of decreased conversion efficiency due to increased ammonia flow rate through the catalyst.

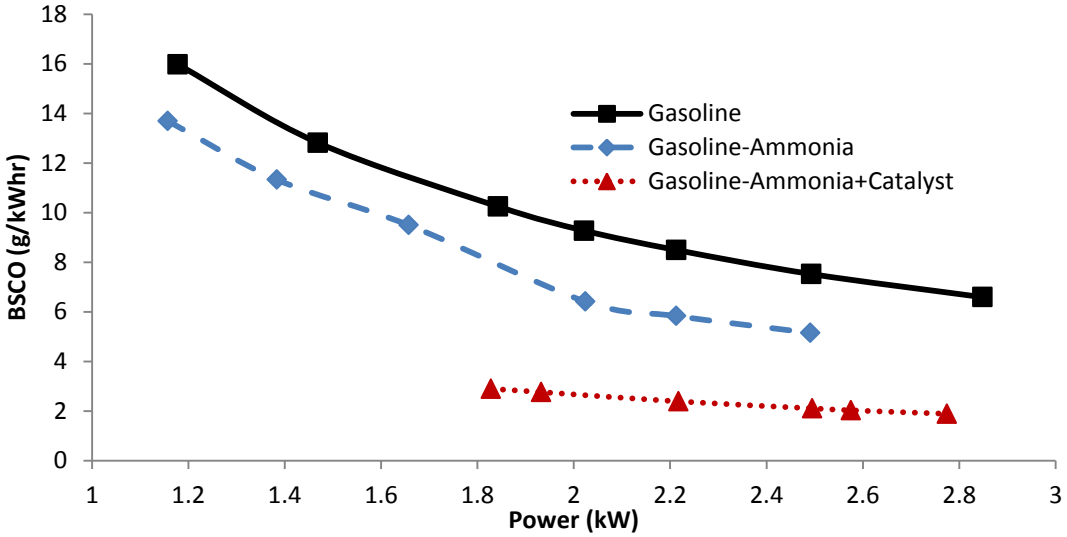

Figure 4.38 BSCO for all fuel cases

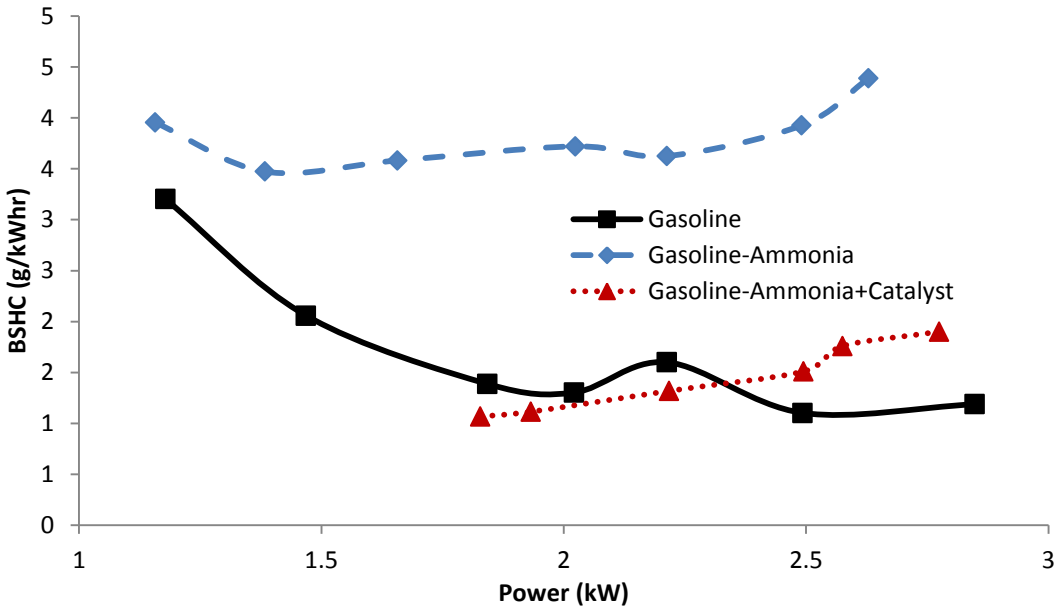

Figure 4.39 BSHC for all fuel cases

The addition of the catalyst has demonstrated promising results for both performance characteristics and emissions data. As can be seen, there are measurable reductions in NOx, NH_3, CO, and HC. There were also improvements demonstrated in performance at low injection durations. These results were diminished as the injection duration increased due to decreased performance of the dissociation catalyst.

Chapter 5 Conclusion

5.1 Liquid Ammonia Direct Injection for CI Engine Application

In this study, appropriate strategies are developed to enable the use of ammonia in direct-injection compression-ignition engines and the corresponding engine performance is evaluated. The effect of fuel mixture composition on engine performance and exhaust emissions in a DI diesel engine using a blend of NH_3 and DME was investigated. Combustion characteristics such as combustion duration, cycle-to-cycle variation, and exhaust emissions including CO, HC, soot, NOx, and NH_3 emissions were analyzed.

Results show that engine speed and load decreases as ammonia concentration in the fuel mixture increases. Significant cycle-to-cycle variations are observed when 40%DME-60%NH_3 is used. However, as the engine load is increased, cycle-to-cycle variations decrease. The maximum brake timing for best torque needs to be advanced with increased ammonia concentration in the fuel mixture due to the high resistance to autoignition of ammonia. Moreover, with the increase in ammonia concentration, both engine speed and engine power exhibit limitations relative to the 100% DME cases. For 40%DME-60%NH_3, the appropriate injection timing is found to range from 90 to 340 BTDC and the engine exhibits homogeneous charge compression ignition (HCCI) combustion characteristics with short combustion duration and low combustion temperature.

When ammonia is used in the fuel mixture, various exhaust emissions increase. For instance, 40%DME-60%NH_3 conditions result in relative high CO and HC emissions at

low load conditions due to the low combustion temperature of ammonia. Soot emissions remain extremely low but are slightly higher than those using 100%DME due also to lower combustion temperature. When ammonia is used, NOx emissions increase due to the formation of fuel NOx. Exhaust ammonia emissions also increase as ammonia concentration in the fuel mixture increases from 40% to 60%. Overall, this study demonstrates that high concentration of ammonia can be used in a DI diesel engine using appropriate injection strategies. Nevertheless, exhaust after-treatment such as selective catalytic reduction (SCR) will be required for reducing gaseous emissions.

Although the results show increased performance for high concentrations of ammonia using highly advanced injection timings it is thought that liquid ammonia direct injection presents significant challenges in achieving 100% ammonia operation. Therefore, it is considered that future approaches will move to gaseous ammonia in order to eliminate cooling effects of ammonia vaporization.

5.2 Gaseous Ammonia Direct Injection for SI Engine Application

Using a CFR engine the ability of gaseous direct injection strategies to increase operating range and performance using ammonia was explored. A gasoline-ammonia combination was used. A ruthenium catalyst was also tested that served to partially decompose the ammonia into hydrogen. The gasoline was delivered through an existing port injection system, while the ammonia was delivered, using a solenoid valve injector, directly to the combustion chamber. The ammonia was delivered in a gaseous state at a

pressure of 13.8 bar. Fuel consumption, performance characteristics, and emissions data were collected to observe the effect of gasoline-ammonia on engine performance.

During the experiments, the CFR engine was initially operated at the idle condition, where idle is considered the minimum amount of gasoline to achieve stable combustion with no other fuel source present. With the engine operating on idle, gaseous ammonia was then directly injected into the combustion chamber and the effects on engine performance and exhaust emissions were characterized. Three ammonia injection timings were tested (270, 320, and 370 BTDC). For each injection timing five injection durations were tested (10, 14, 18, 22, and 26 ms). Based on the results, seven performance modes were determined based on the following flywheel powers: 1.25, 1.50, 1.75, 2.00, 2.25, 2.50, and 2.75 kW. The performance modes were achieved using gasoline and gasoline-ammonia in order to compare performance parameters and emissions data of both fuel scenarios. Using identical injection timings and durations a ruthenium catalyst was added in order to compare the effects of the addition of the catalyst on engine performance and exhaust emissions.

Flywheel power, pressure traces, heat release rate histories, and emissions data, including NH_3, NOx, CO_2, CO, and HC, were collected for performance modes using gasoline, gasoline-ammonia, and gasoline-ammonia with a ruthenium catalyst.

Results show that using gasoline-ammonia little improvement of BSEC or CO_2 is observed. It was also observed that that there was a significant increase in both NOx and HC. It was also observed a slight decrease in CO production. It is thought that the ammonia slightly inhibits combustion causing decreased CO and increased HC. It is

expected that CO_2 should also be decreased with gasoline-ammonia. However, little improvement was observed. It is thought that because the full throttle condition of the CFR engine required a large amount of fuel to achieve idle condition that the ammonia does not reduce CO_2 levels by a noticeable amount relative to the amount of CO_2 produced at idle condition.

The addition of ruthenium catalyst to partially decompose ammonia into hydrogen showed measurable improvements in performance and exhaust emissions over gasoline-ammonia without a catalyst. Using identical injection timing and duration it was seen that for low to medium injection duration with the catalyst present there was an increase in flywheel power. Based on injection temperature it was concluded that for low to medium injection duration (low ammonia flow rate through the catalyst) the catalyst was successful in dissociating an appreciable percentage of ammonia into hydrogen. For high injection duration (high ammonia flow rate through the catalyst) the effects were minimal, thus suggesting that for high flow rates the catalyst was insufficient in surface area and residence time to dissociate a larger quantity of ammonia.

With the use of a catalyst, it was observed that the in-cylinder peak pressure was increased and the start of ignition was advanced. It is thought that the presence of hydrogen in the fuel mixture promoted ignition and enhanced combustion and due to hydrogen's high flammability limit and high flame speed.

The use of a catalyst also helped significantly reduce NH_3 and NOx emissions in the exhaust. Increased combustion efficiency and reduced fuel-bound nitrogen are

thought to cause the reduction of NH_3 and NOx. The catalyst also showed equivalent levels of HC as gasoline and improved CO emissions over gasoline. Both improvements are attributed to increased combustion efficiency due to the presence of hydrogen.

Based on the results of this project, it is concluded the current technologies on the market does not make gaseous ammonia direct injection a viable approach. More work is required to further examine gaseous direct injection using more advanced mechanical equipment. Promising results were seen with the addition of a ruthenium catalyst. Further work is needed to examine the surface area and residence time required to supply a sufficient percentage of hydrogen to the combustion chamber in order to see results at all flow rates of ammonia.

Chapter 6 Works Cited

[1] "The World Factbook," Central Intelligence Agency, 30 January 2013. [Online]. Available: https://www.cia.gov/library/publications/the-world-factbook/geos/xx.html. [Accessed 5 Febraury 2013].

[2] C. Zamfirescu and I. Dincer, "Using ammonia as a sustainable fuel," *Journal of Power Sources,* no. 185, pp. 459-465, 2008.

[3] B. D. Joseph, "Solid State Ammonia Synthesis (SSAS) for Sustainable Fuel and Energy Storage Applications," Colorado School of Mines, Physics Department .

[4] C. W. Gross and S.-C. Kong, "Performance characteristics of a compression-ignition engine using direct-injection ammonia-DME mixtures," *Fuel,* vol. 103, pp. 1069-1079, 2013.

[5] C. Morch, A. Bjerre, M. Gottrup, S. Sorenson and J. Schramm, "Ammonia/hydrogen mixtures in an SI-engine: Engine performance and analysis of a proposed fuel system," *Fuel,* vol. 90, pp. 854-864, 2011.

[6] C. Zamfirescu and I. Dincer, "Ammonia as a green fuel and hydrogen source for vehicular applications," *Fuel Processing Technology,* no. 90, pp. 729-737, 2009.

[7] "Fuel Gage Report," AAA, 4 Febraury 2013. [Online]. Available: http://fuelgaugereport.aaa.com/?redirectto=http://fuelgaugereport.opisnet.com/index.asp. [Accessed 4 Febraury 2013].

[8] "Mineral Commodity Summaries," U.S. Geological Survey, 2013.

[9] S. Badcock, "Clean Citites Alternative Fuel Price Report," U.S. Department of Energy , 2012.

[10] "Emission Standards Reference Guide," United States Environmental Protection Agency, 18 December 2012. [Online]. Available: http://www.epa.gov/otaq/standards/index.htm. [Accessed 5 Febraury 2013].

[11] W. Wang, J. M. Herreros, A. Tsolakis and A. P. York, "Ammonia as Hydrogen Carrier for Transportation; Investigation of the Ammonia Exhuast Gas Fuel Reforming," *Environmental Science & Technology,* 2012.

[12] S. Frigo, R. Gentili and N. Doveri, "Ammonia plus hydrogen as fuel in a S.I. Engine: Experimental Results," *N/A,* p. N/A, N/A.

[13] E. Morgan, J. Manwell and J. McGowan, "WIND-POWERED AMMONIA FUEL PRODUCTION FOR REMOTE ISLANDS," American Solar Energy Society, 2013.

[14] J. R. Bartels and M. B. Pate, "A feasibility study of implementing an Ammonia Economy," Iowa State University , 2008.

[15] P. Brown, "U.S. Renewable Electricity: How Does Wind Generation Impact Competitive Power Markets?," Congressional Research Service, 2012.

[16] W.-y. Huang, "Impact of Rising Natural Gas Prices on U.S. Ammonia Supply," Economic Research Service , 2007.

[17] E. Kroch, "Ammonia-A Fuel for Motor Buses," *J Ins Petrol,* no. 31, pp. 213-223, 1945.

[18] A. J. Reiter and S.-C. Kong, "Demonstration of compression-ignition engine combustion using ammonia in reducing greenhouse gas emissions," *Energy Fuels,* no. 22, pp. 2963-2971, 2008.

[19] A. J. Reiter and S.-C. Kong, "Combustion and emissions characteristics of a compression-ignition engine using dual ammonia-diesel," *Fuel,* no. 90, pp. 87-97, 2011.

[20] T. Pearsall and C. Garabedian, "Combustion of anhydrous ammonia in diesel engines," *SAE paper 670947,* 1967.

[21] S. M. Grannell, D. N. Assanis, S. V. Bohac and D. E. Gillespie, "The Fuel Mix Limits and Efficiency of a Stoichiometric, Ammonia, and Gasoline Duel Fueled Spark Ignition Engine," *Journal of Engineering for Gas Turbines and Power,* vol. 130, no. 042802, 2008.